Volume 46, Number 2, 2020.

Mobility & Vehicle Mechanics

International Journal for Vehicle Mechanics, Engines and Transportation Systems

ISSN 1450 - 5304

UDC 621 + 629(05)=802.0

UNIVERSITY OF KRAGUJEVAC, FACULTY OF ENGINEERING

SERBIAN SOCIETY OF AUTOMOTIVE ENGINEERS

M V M Mobility Vehicle Mechanics

Editors: Prof. dr ***Jovanka Lukić****; Prof. dr* ***Čedomir Duboka***

For Publisher: Prof. dr Dobrica Milovanović, dean, University of Kragujevac, Faculty of Engineering

Publishing of this Journal is financially supported from:
Ministry of Education, Science and Technological Development, Republic Serbia

Mobility & **V**ehicle **M**echanics

Volume 46
Number 2
2020.

Motorna **V**ozila i **M**otori

Mobility & **V**ehicle **M**echanics

Volume 46
Number 2
2020.

Motorna **V**ozila i **M**otori

MOBILITY & VEHICLE MECHANICS

DOI:10.24874/mvm.2020.46.02.01
UDC: 629.025

FORMULA SAE REAR SUSPENSION DESIGN

*Tarun Kumar[1], Roger Stephen[2], Mohammad Zaeimi[3] and Greg Wheatley[4]**

Received in May 2020 Accepted in June 2020

RESEARCH ARTICLE

ABSTRACT: The purpose of this report is to investigate the design development and evaluate the structural and functional performance of the proposed system for the 2019 competition. With the review of the literature surrounding rear suspension systems, FSAE standards, analysis techniques and important design parameters, the foundation for the proposed James Cook University (JCU) 2019 rear suspension system is established.

This paper is highlighted the development and analysis path undertaken in the construction of rear suspension system befitting a Formula SAE vehicle. Formula SAE is an international student competition centered on the design, construction and racing of an internal combustion vehicle. All parts are designed via SolidWorks and FEA testing is incorporated using ANSYS to test out various loads under different scenarios in racing. Main components including beam axle, trailing arms, brackets, spring and damper are covered in this paper. The design is focused on providing a low cost and easy to manufacture design which operate for infinite life cycles.

KEY WORDS: Rear suspension design, Dependent suspension system, Formula SAE suspension, steering, design, finite element analysis

[1] *Tarun Kumar , BSc, College of Science and Engineering, James Cook University, Townsville, Australia*
[2] *Roger Stephen, BSc, College of Science and Engineering, James Cook University, Townsville, Australia*
[3] *Mohammad Zaeimi, MSc, Young Researchers and Elites Club, Science and Research Branch, Islamic Azad University, Tehran, Iran*
[4] *Greg Wheatley, College of Science and Engineering, James Cook University, Townsville, Australia, greg.wheatley@jcu.edu.au (*corresponding author)*

PROJEKAT ZADNJEG OSLANJANJA FORMULA SAE

REZIME: Svrha ovog rada je da prikaže istraživanje, razvoj i procenu strukturnih i funkcionalnih performansi sistema predloženog za takmičenje 2019. godine. Pregledom literature o sistemima zadnjeg oslanjanja, FSAE standarda, tehnika analize i važnim projektnim parametrima, formirana je osnova za predloženi sistem zadnjeg oslanjanja Univerziteta James Cook (JCU) 2019.

U ovom radu je prikazan razvojni put i analiza koja je urađena u konstrukciji sistema zadnjeg oslanjanja vozilu Formule SAE. Formula SAE je međunarodno studentsko takmičenje fokusirano na dizajn, konstrukciju i trke vozila sa motorom sa unutrašnjim sagorevanjem. Svi delovi su dizajnirani pomoću SolidWorks-a, a FEA testiranje opterećenja u različitim scenarijama trka je urađeno pomoću ANSIS-a. U radu je prikazan razvoj glavnih delova, uključujući: krutu osovinu, vođice, nosače, oprugu i amortizeru. Fokus dizajn je na niskim troškovima proizvodnje i jednostavnom proizvodnom procesu sistema koji treba da ima beskonačan životni ciklus.

KLJUČNE REČI: Razvoj zadnjeg oslanjanja, Zavisan sistem oslanjanja, Oslanjanje Formule SAE, Upravljanje, dizajn, Analiza konačnim elemenatima

FORMULA SAE REAR SUSPENSION DESIGN

Tarun Kumar, Roger Stephen, Mohammad Zaeimi, Greg Wheatley

1 INTRODUCTION

he Formulae Society of Automotive Engineers (FSAE) competition is bounded by a strict set of rules that must be adhered to by all competing teams. These rules are enforced to ensure the safety of all involved, whilst also placing limits on vehicles, creating an even playing field. Moreover, other constraints including considerations of material, geometry and manufacturing processes should also be taken into account [1].

A motor vehicle's suspension system creates the harmony between road and the driver orchestrating all the components of the chassis that need to work together, the suspension system stabilizes the vehicle attitude during accelerating, breaking and cornering while isolating road's roughness from passenger compartment. Suspension system is the link between the wheels and the chassis, transmitting the weight of the vehicle on to the wheels. A suspension system must keep the wheels in proper camber, resist chassis roll to an extent and keep the tires in contact with the road surface with minimal load variations for the vehicle to handle in a desirable manner.

Selecting the correct suspension design for an application is of crucial importance and usually compromises are required, whether it is in the geometry to allow for more space in the car or in the stiffness of the ride to accomplish the necessary handling characteristics – planning a suspension system is a significant task while designing a desired car. There are various factors which are required to be analyzed in the development for the design of the suspension of a motor vehicle. Some major factors include, independent or dependent systems, camber, and toe, roll center etc.

According to the FSAE Design Event Score Sheet [1], with the majority of marks associated with the dynamic performance of the car, therefore, therefore, it is imperative that the suspension of the vehicle is a competitive solution and can withstand the entirety of the events.

With the review of the literature surrounding rear suspension systems, FSAE standards, analysis techniques and important design parameters, the foundation for the proposed James Cook University (JCU) 2019 rear suspension system is established. The purpose of this report is to investigate the design development and evaluate the structural and functional performance of the proposed system for the 2019 competition.

The rest of this paper is organized as follows. In Section 2, independent and dependent suspension systems are introduced. Preliminary considerations, including design constraints and load conditions, and design development are proposed in section 3. Numerical analysis of the proposed system is presented in Section 4. Finally, in Section 5, conclusions are presented.

2 SUSPENSION SYSTEM

The main objective of the current work was to design a low cost and easy to manufacture suspension system with an appropriate performance. Considering this, the optimum choice was between a dependent system and an Independent system and to save money and cost. There are a range of suspension systems utilized by various teams in the FSAE competition. Suspension systems can be categorized into two main systems, namely independent suspension and dependent suspension.

2. 1 Independent rear suspension

Independent suspension refers to the rear suspension system of the vehicle which allows each wheel to move independently from one another. Independent rear suspension (IRS) systems are preferred in vehicles where comfort and performance are major requirements. The MacPherson Strut [2] and the Double wishbone [3] are two commonly configurations; however, the most common IRS setup used in racing situations such as FSAE is double wishbone [4-6]. A double wishbone uses two wishbones where each wishbone is made of two single arms which have their two ends joined together to create a V shape and a trailing arm to attach the upright to. Factors such as control arm length and mounting, camber and toe settings, roll center, pitch center and center of gravity should be considered thoroughly to construct reliable and effective rear suspension [7, 8].

Independent suspension involves complex geometries, increased costs and maintenance. Designing a successful double wishbone can greatly improve the vehicles handling, traction, and stability and ultimately dictate the success of the vehicle. However, there are many moving parts which must be accurately and precisely engineered so that geometries are exactly as designed. An error in the geometry can have detrimental effects on the vehicle's performance and driver's safety. A well rounded system may take multiple stages of development and multiple redesigns which can be very costly and time consuming. With increased components comes increased weight and costs. The wishbones, pushrods and sway bar will take up tremendous space at the back of the vehicle and will add a substantial amount of weight to the car. With space being already scarce on FSAE vehicles, and to improve performance; a smaller lighter unit will need to be developed. This will be a costly venture which may not be beneficial as shortened geometries can lead to reduced effectiveness.

2. 2 Dependent rear suspension

Dependent suspension systems have a rigid linkage between the two tires, such that any movement of one wheel is translated, and thus the forces are also translated from one wheel to another. Non-independent suspension system has the advantages of simple structure, low cost, high strength, and easy maintenance. As mentioned before, the aforementioned independent systems all have better handling and more effective but the many of these advantages have to be overlooked due to the cost effectiveness of beam axles. Therefore we decided to go with dependent system, more specifically, a solid/rigid axle.

There are different types of suspension setup including leaf springs [9], there-link [10] and four-link [11] systems. The solid axle consists of the basic dependent system where the two rear wheels relate to a form of a rigid beam, so that when one-wheel encounters and irregularity on the track surface, the other wheel is directly affected. This type of suspension is usually found on the rear of a rear-wheel drive and is therefore a live axle. The translation of forces between the connected wheels causes the camber angle to be consistent regardless of the travel of the suspension. A solid axles' fore and aft location is constrained by either trailing arms, semi-trailing arms, radius rods or leaf springs. The lateral location is constrained by either a paint hard rod, a Scott Russell linkage or a Watts linkage. Solid axles have two instant center axes, one for parallel bump motion and the other for roll, these axes will move with changes in ride height [12].

The principal advantage of the solid axle is the simplicity causing it to be very space efficient and relatively cheap to manufacture, also it is extremely strong and durable, making it a suitable fit in high load environments. Drawbacks for this type of suspension is that it does not allow each wheel to move independently in response to bumps and the mass of the beam is part of the unsprung weight of the vehicle which can further reduce ride quality. The cornering is inferior than other suspension designs as the wheels have zero camber angle gain during body roll, furthermore, front solid axle suspension is unusually sensitive to any lack of concentricity in the hub and wheel assembly which can cause a side to side oscillation.

3 DESIGN APPROACH

The design of the suspension system was focused around three key objectives, it was essential to achieve infinite life cycles, high strength to weight ratio, and to reduce the total cost to manufacture and assemble the vehicle. The design process of the vehicle suspension has been based on iterative experimentation approaches, where design variables (e.g. material, geometry, damping, etc.) have been altered, and re-analyzed the system until acceptable design criteria's have been achieved.

3. 1 Preliminary considerations

Load cases

It is essential to consider multiple load cases for different scenarios of the vehicle as forces in each suspension member are different given the geometry and orientation of the system. Force analysis is an integral part of any FSAE team and must be completed as part of the FSAE Structural Requirements Certification Form (SRCF) [1]. Whilst there are a number of load scenarios that may be considered for analysis, of which would be subjected to the car during static and dynamic events, only the critical load cases will be analyzed. These critical load cases include linear acceleration, braking and critical cornering in this work. Understanding the forces and stresses within the suspension components allows effective design iterations to be made to later redesign geometry for a better performance.

Numerous assumptions need to be made to ensure the accuracy of force calculations and the transmission of forces through the vehicle components. It is essential to assume that the rigid links connect the center of mass (COM) to the tire contact points and the resulting force acts through the suspension geometry. Therefore, the forces generated by the different load cases transmit through the tire contact patch to the upright and to the mounting surfaces of the rear axle. Whilst the forces are transmitted to the mounting face between the upright and rear axle, the location of the force is the center of the tire. Hence throughout the analysis, remote forces at this location are used to account for the force and moment generated. Additionally, as the coefficient of friction between the tire and the track is constantly changing due to the heat generated at the contact point, the coefficient was 0.8 which was verified throughout literature. This value was used to determine the frictional force on the wheels for the different load cases.

For the linear acceleration and braking load cases, specialized formulas were used to develop loads based on the vehicle parameters in table 1. The calculations for these different load cases provide an estimation of the forces acting in each direction on the suspension and would require physical testing to improve accuracy.

Table 1 Vehicle parameters

Parameter	value
Linear acceleration	1 g
Braking	1 g
Mass of car	400 kg
Wheelbase	1630 mm
Centre of Mass Height	350 mm

Coefficient of Friction	0.8

Linear acceleration

An important load case to consider for the FSAE vehicle is routine linear acceleration which occurs frequently during the dynamic events. From ref [1], the acceleration event involves the evaluation of the vehicle's acceleration in a straight line on flat pavement across 75m. For this load case it is assumed the acceleration is purely linear as it travels down the track. The maximum acceleration of the vehicle for critical acceleration is considered to be $1.019\ g$ which corresponds to $10\ m/s^2$. As purely linear acceleration is being analysed for this load case without any affect from braking, the force is considered a zero-based, cyclic load. During linear acceleration, the $\mathrm{F_z}$ (forward direction) component of the rear suspension is due to the tractive forces on the rearward tires. The $\mathrm{F_x}$ component of the vehicle is zero as the acceleration is purely linear, and no cornering is experienced. In addition, forces in the y direction are comprised of the static weight of the vehicle and driver on the wheels and the dynamic weight transfer from front to rear caused by the acceleration. These forces can be calculated with the equations proposed by Smith [8] (see Appendix A).

Braking

Another very common occurrence during the racing of the FSAE vehicle is specifically linear braking, experienced when slowing down [1]. The maximum braking force is a function of the deceleration in the z component, which was considered a maximum of 1 g without the wheels locking up. Like the linear acceleration, the F_x component will be zero as there is no cornering. The force in the y direction is due to the static weight on wheels less the dynamic weight transfer as the braking occurs and the weight shifts forward. Using the vehicle parameters in table 1, the braking forces for each component are determined from the formulations in ref [8] (see Appendix A).

Critical Cornering

To incorporate all the forces acting on the car at once during a scenario, a load case has been developed for the critical cornering whilst braking. This case can be considered a worst-case scenario and is essential for analysis to determine the performance of the suspension under loading configurations. This scenario is subjective, with some papers considering this to be the forces experienced while cornering at maximum deceleration, see Figure 1 [13], while others consider it to be merely a maximum cornering effect, whereas the suspension is fully compressed on one side and fully relaxed on the other [14].

The free body diagram in Figure 1 displays the information for the applied loads during critical cornering of the car. There are numerous assumptions associated with this load case, which stipulate that the vehicles performance is $1.2\ \mathrm{g}$ cornering acceleration and $10\ \mathrm{m/s^2}$ straight line acceleration. In addition, it is assumed that rigid links connect the COM to the tire contact points and the resulting force acts through the suspension geometry.

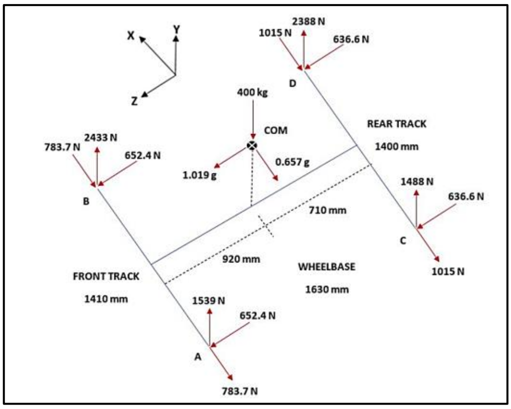

Figure 1 Critical load case [13]

From this set of information, the critical forces were identified, and forces produced from the tires to the rear axle and the direction of the forces were used to develop the load case. During cornering, the weight naturally transfers from the outside to the inside wheel, which creates a moment with respect to the origin.

On the other hand, the suspension will resist this moment through the various components designed to counteract the motion and hence generate the reactive force. As the vehicle takes alternative corners, the direction of the loads changes and hence the load is analyzed as a fully reversed, cyclic load.

Table 2 Summary of load case forces

Load Case	F_x	F_y	F_z
Linear Acceleration	0	1528.28 N	1222.4 N
Braking	0	658.76 N	54861 N
Critical Cornering	1015 N	2388 N	636.6 N

From the critical loading case of the entire vehicle, the loads for the rear suspension quarter can be applied to the geometry. The 1.019 g force acts on all components whilst the X, Y and Z forces from the tire act on the mounting surface of the rear axle. With the loading specifications sourced directly from the client and calculated using reliable sources, the accuracy of the loading conditions are assured. A summary of the loads in each direction acting on the rear axle during critical load cases is presented in Table 2. These forces are used for the FEA investigation to analysis the performance of the rear suspension and inform design changes.

3. 2 Constraints of the design

The design of any component should be undertaken with the goals of satisfying the technical requirements set by FSAE 2019 rules (e.g. geometry restrictions on the size of wheelbase track and ground clearance, fasteners, etc.) [1] and constraints arise from facility limitations and considering the main objective of the design including low cost and easy to manufacture suspension system. For this purpose, the following considerations were performed.

Material selection is one of the first key factors for all FSAE teams when designing components for the suspension system. The first and most important consideration taken when selecting the suspension system material is its strength to weight ratio. Aluminum, composites and carbon tubes are examples of such materials that possess a good ratio. However, these materials are generally far more expensive and more difficult to process [13]. Due to this a compromise is generally made and therefore common materials used for structural members are Chromalloy and mild steel. These material's strength to weight ratio is still fairly good compared to Aluminium composites and carbon tubes. Chromalloy and steel are easy to handle and relatively cheap. A comparison of several possible material selections can be seen below in Table 3. Therefore, we decided to set 4130 Steel for the beam axle, trailing arms and mild steel for the brackets and weld-in bung.

Table 3 Material Advantages and Disadvantages [13]

Material	**Advantages**	**Disadvantages**
Mild Steel	• Baseline material requiring no additional design • Easy to weld • Good workability	• Mild steel tube not readily available locally in small quantities.
AISI 4130	• High strength • Easy to weld • Can be sourced for a reasonable price	• Requires interstate delivery • Material weakens when welded • FSAE rules state minimum tube size
Composite	• Very high strength to weight ratio	• Requires proof build quality • Very expensive • Needs monocoque designs • Requires mechanical fastening to main hoop
Aluminium	• Good strength to weight ratio • High workability	• Requires Mechanical fastening to the main hoops • Best used in monocoque designs • Difficult to source locally

Additionally, according to all relevant FSAE standards, ensuring no component of the suspension clashed with external components of the vehicle is essential. This involved designing the suspension to avoid the drive train, differential and CV shafts whilst static and during vertical travel of the suspension. To ensure this, regions specifying the locations where the brackets could be mounted to the frame to support the trailing arms should be identified accurately.

Based on budget limitation, the type and size of the shocks to be used for the suspension was specified in the preliminary design. Along with an effective suspension geometry, selecting the correct springs and shock absorbers is essential to maximize the tire contact with the road surface. Consequently, it will result in an increase in traction of the vehicle which will enable the car to travel at higher speeds more safely [15]. It is decided to use Penskie 7800 shocks with with a spring length of 200 mm and spring stiffness of 57 N/mm.

Moreover, to reduce the overall weight and consequently the cost, it essential that the geometry of the suspension is compact and many external components are avoided, yet structurally sufficient. In addition, the proper movement of the suspension system in response to dynamic loads is critical to ensure the optimal performance of the vehicle. This involves ensure the roll centre is adequately design with consideration of the trailing arm geometry. Further, the beam axle must be allowed to effectively rotate as it travels to allow the transfer of loads thought the suspension. This ensures that the rod ends and trailing arms are not placed in significant bending, which is to be avoided. Finally, the suspension system could be design to operate as required for dynamic events. Whilst under loads caused by acceleration, braking and cornering, the suspension is required to support the load of the vehicle whilst maximizing the tire contact. To allow this movement, trailing arms are required to be mounted to the frame and the rear axle which support the wheels.

This was the basis for the preliminary design and further development was achieved through iteration processes based on informed analysis.

3. 3 Design development

Beam axle

There were two options for the design of the beam axle, a single beam across the rear chassis connecting to the two-wheel uprights, or a double beam side by side which are smaller in diameter. The latter option was a method to reduce the space taken vertically to avoid any potential clashes in geometry, however, after incorporating the wheel diameters, it was found that there was enough clearance to just use one beam with a larger diameter.

The initial design consisted a 50 mm diameter beam with 3 mm thick walls. Multiple brackets were created for this design and attached to the beam geometry to start testing. There were two options to adjust toe as follows. The first one was to incorporate ball joints, which are two plates with ball bearings roaming free between them. For this purpose, the hub shaft would have to be thicker and too many parts would need to be altered for a simple toe adjustment on race day. Another possible option was the use of shims which were incorporated in the wheel hub because of ease of implementation.

After testing, it was found that the diameter and thickness of the beam should be updated to 30 mm and 6 mm respectively to tackle the increased forces when under critical loads. The weight difference between the two beams were considered negligible relative to the increased strength of the beams. It should be noted that the mounting brackets have been tilted 30 degrees towards the front of the car to avoid obstructing the CV shaft when it under full compression.

Moreover, the weld-in bund was developed to allow integration between the upright and the beam axle. The weld-in bung is welded to the axle and to a bracket which is then bolted to the upright to support the wheel assembly. The rigid connection between the upright and the axle allows the tire contact forces to transmit through the wheel assembly and are dispersed through the circular tubing and suspension components.

Training arms

Figure 2(a) shows the preliminary geometry of the mild steel trailing arms attached to the beam axle, it used a parallel geometry for the arms and connected to the beam using bolts. The arms were imported to the main assembly for the vehicle and it was at this point a glaring issue was identified.

SolidWorks has a very convenient feature to observe points such as instantaneous centers and roll centers. Not that the roll center is the point where the loads experiences at the tire patches act on the sprung mass of the system. Its position with respect to the center of gravity dictates how much rolling moment the system will experience while cornering. Essentially, lowering of the roll center will result in a higher rolling moment while cornering and influences the turning radius of the vehicle. Further effects of a higher rear roll center include, higher responsiveness in cars when coming in and out of corners, and advantageous to use on high grip conditions, such as tracks, to avoid traction rolling. It was found that with the parallel arm geometry with equal lengths, the roll center remained close to the ground.

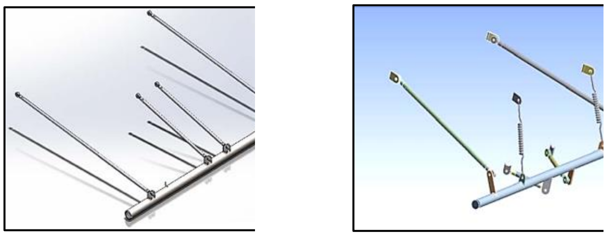

(a) (b)

Figure 2 Trailing arm: (a) initial geometry and (b) final geometry

To combat this issue and have a higher roll center, the arms are angled in from the chassis to the beam axle. With the trailing arms angled in the design of the suspension geometry, any axial loads on the beam axle are transferred to compressive and tensile forces through the arms. This avoids undesirable bending within the trailing arms and provides a reduction in stress.

In addition to this, the lower arms are much shorter in length, causing a change in camber of the vehicle as it rolls, helping it to keep the contact patch square on the ground, increasing the ultimate cornering capacity of the vehicle. It also reduces the wear of the outer edge of the tire. FEA testing was performed on this short-long arms design, and it was found that cornering forces are higher and therefore stiffer bushings are required at the body. The arms have been designed with spherical bearings for all attachment points. This maintains all forces transferred in line with the bearings, eliminating unnecessary moments. With the thoughtful design of the suspension geometry, the trailing arms and rod ends used for the system are readily available, off the shelf components. With reduced stresses present, cost effective components can be utilized without compromising structural performance.

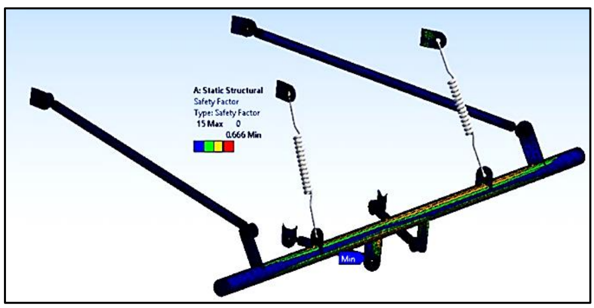

(a)

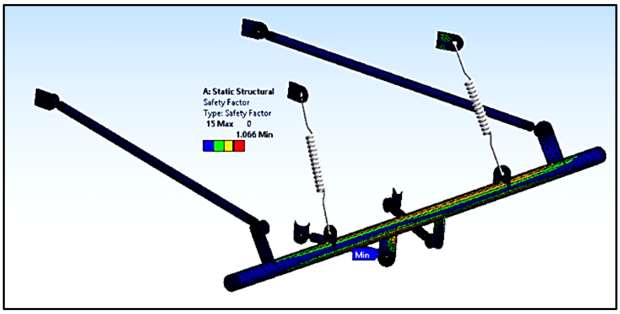

(b)

Figure 3 Safety factor of the space frame made of (a) steel and (b) Chromoly

Mild steel in the same wall thickness, as a Chromoly tube, is said to be almost half the strength in terms of tensile and torsional resistance. The high strength to weight ratio makes Chromoly desirable for applications where weight saving is essential, such as aerospace components and race car parts. It can easily be machined using conventional methods and the welding of the material can be performed by all commercial methods. The difficulty with Chromoly is with respect to its costing, especially for those where the budget is heavily constrained. Keeping this in mind, the design team recommends using Chromoly for the beam axle and the trailing arms, as this allows the component to have the required structural integrity while reducing the weight by 42%.

As shown in Figure 3(a), using the mild steel beam results in heavy stresses acting on the arms. The life cycle on this arms is said to be finite and this is not a desired outcome when designing a dynamic part with a great consideration to performance and safety, especially due to the fact that reusing the model in future years is a very desirable outcome. In contrast to the previous beam material, form Figure 3(b), FEA results indicate an infinite life cycle and a minimum safety factor of 1. Note that a spring was used in the FEA analysis to replace the shocks and replicate the reaction force counteracting the travel of the suspension during loading.

Bracket

When modelled with our critical forces, which is the loads calculated when the car is cornering, there are some stress concentrations on the edges of the bracket where the trailing arms are connected.

A stress concentration is defined as a high localized stress, compared to the average stress of the body, and is typically found in a region that has an abrupt geometric change. They will be in the small radii and sharp corners that are in a load path. The max von Mises equivalent stress was 311 MPa, which is well below the yield strength of Chromoly, but not low enough for our brackets to have infinite life. An investigation was undertaking to reduce the force flow around the notch to solve this issue.

As mentioned in ref (Wiley and sons), stress concentration factor, is a dimensionless factor that is used to quantify how concentrated the stress is in a material. It is defined as the ratio of the highest stress in the element to the reference stress, the graphs provide minimum radius lengths of a fillet when there is a connection between varying diameters. As presented inFigure 4, incorporating this concept of fillets smooth out the stress flow lines and along with applying a concentrated mesh at the max point provided more accurate and improved values. The new von Mises stress was 91 MPa, well below the yield strength and therefore had an infinite life cycle, rendering this design iteration as very successful change.

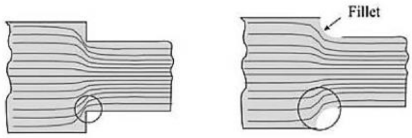

Figure 4 Stress concentration diagram

The water jet cutting was used for the brackets because it offers manufacturers flexibility that no other cutting process can offer. It is preferred over CNC milling as it is a more accurate form of manufacturing and this is vital as the filleted corners need to be as smooth as possible to mitigate any stress concentrations.

Shocks

The spring and damper are mounted directly to the chassis of the vehicle, and this configuration reduces unsprung weight and improves the response of the suspension system. The suspension system uses coil over springs where the springs are mounted to the outside of the damper with an adjustable preload on the spring to adjust the ride height of the car. This allows the design to be attentive on performance over comfort and directs the optimization of the handling of the vehicle. With the spring stiffness increasing the stiffness of the suspension coupled with a low center of gravity, the vehicle can be controlled significantly easier.

3. 4 Final design

Depicted below in Figure 5, the rear suspension system is designed within FSAE and Australian Standards and adheres to the predefined constraints and limitations. It is structurally sufficient and thoughtfully developed to ensure adequate scoring during FSAE static and dynamic events. As mentioned before, the final design features 30mm diameters Chromoly beam axles with a tubing thickness of 6mm. It is equipped with direct acting Penskie 7800 shocks with spring stiffness of 57 N/mm. The trailing arm geometry is positioned to optimize the position of the roll center to allow better performance of the vehicle.

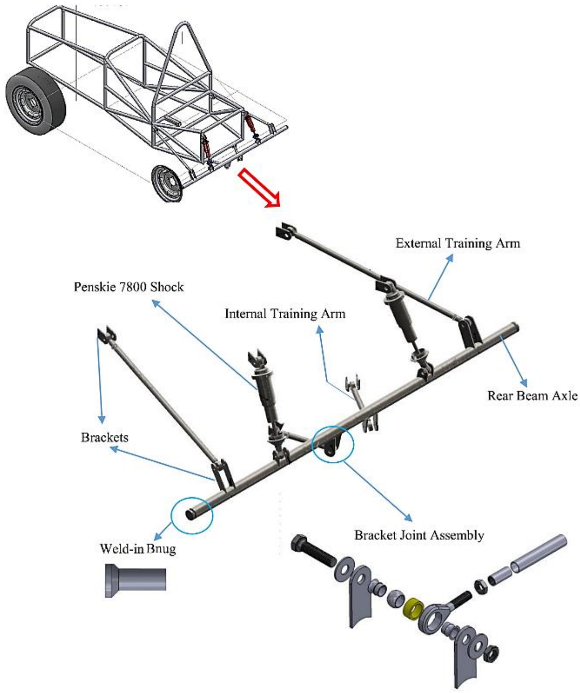

Figure 5 Final suspension design schematic

4 NUMERICAL ANALYSIS

Before manufacturing processes, Finite element analysis (FEA) can be used to represent the complex geometry and simulate the forces transmitted to the model with equivalent boundary conditions. In this way refinements can be made and rapidly assessed for a small fraction of the cost of prototyping and experimental testing. The FEA method is utilized through ANSYS static structural modelling of equivalent stress and total deformation in the vehicle's rear suspension.

Moreover, since the rear suspension components are critical elements of the vehicle system which are subjected to a cyclic loading, a fatigue analysis must be conducted with realistic endurance limit modifying factor. It was conducted in ANSYS using the fatigue tool which analysed the stress life using the Goodman equation. The cyclic loading generated by the load cases is equivalent to zero based loading for purely linear acceleration and braking and fully-reversed for the critical cornering case, with the endurance factor of 0.67 (see Appendix B) calculated from ref [16]. Given the material properties of each suspension component, this analysis provides an expected life and safety factor of the mechanism based on the limiting factors specified. To design the components for infinite life, the suspension is expected to exceed 10^6 loading cycles.

4. 1 Linear Acceleration

With the forces developed for the linear acceleration load case, the structural performance of the rear suspension was analyzed in ANSYS. Figure 6 demonstrates the stress profile throughout the beam axle and trailing arms, identifying the maximum stress location at the rod ends. The maximum Von Mises stress recorded in the rear suspension was 174.15 MPa. With the minimum fatigue limit of materials used for the components being 220 MPa for mild steel, the safety factor of the system is 1.26. Therefore, it is expected that under linear acceleration the rear suspension would operate for infinite life.

From the stress concentration, it is clear that the beam axle has area of high stress, specifically around the bracket mounting locations. However, with the beam axle tubing constructed from 4130 Steel, the strength is more than sufficient to withstand these stresses. In addition, from the FEA analysis, the vertical travel of the suspension during linear acceleration was determined to be 28.12 mm. This resulted in a counteractive spring force of 1602 N provided by the shocks.

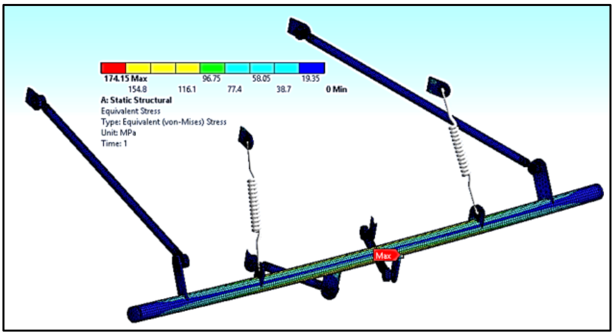

Figure 6 Stress concentration for linear acceleration load

4. 2 Braking

With the weight transfer towards the front of the vehicle during braking, it is expected that the loads and resulting stress in the rear suspension is reduced, when compared to acceleration. As proposed in Figure 7, the resulting stress profile identified a maximum von Mises stress of 157 MPa, located within the rod ends.

With similar loads applied, the resulting stress profile resembled that of the linear acceleration cases, with only a minor reduction in stresses. With the maximum stress significantly below any of the materials fatigue limit, the safety factor of the suspension system during braking was a minimum of 1.4. Consequently, all the components are operating within the limit of infinite life. Since the maximum stress significantly below any of the materials fatigue limit, the safety factor of the suspension system during braking was a minimum of 1.4. Consequently, all the components are operating within the limit of infinite life. Under this load case, the vehicle travel of the suspension was measured as 9.24 mm, with a resulting shock force of 527 N.

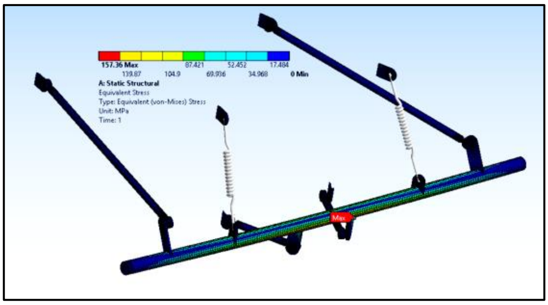

Figure 7 Stress concentration for braking load

4. 3 Critical Cornering

The final and most critical scenario considered for analysis was maximum cornering whilst accelerating, based on the load case previously developed for high-speed cornering situations. The stress profile for the suspension under this loading configuration is displayed in Figure 8.

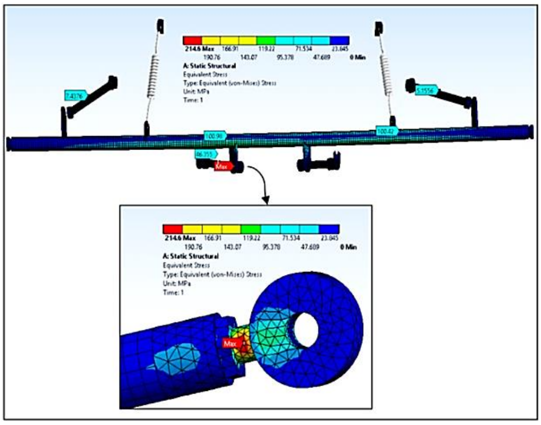

Figure 8 Stress concentration for critical cornering load

With stress probes used to demonstrate key values. This figure demonstrates the stress concentration along the Chromoly beam axle and within the trailing arms. With the maximum stress of 214.6 MPa identified in the rod ends, the other stress concentrations highlighted along the beam axle are significantly lower. In addition, with the use of a spring probe, the travel of the suspension for critical cornering was determined to be 62.27 mm, producing a force in the shocks of 3549 N.

Figure 9(a) demonstrates the safety factor of a number of suspension components, with the minimum safety factor identified in the rod ends of 1.066. For the beam axle, the safety factor ranges from 1, in areas of high stress, to 15, where the stress concentration is minimal. In addition, it was observed that the trailing arms has limited stress throughout them, leading to a significantly high safety factor approximately 15, for the majority of the length. Further analysis of the rear suspension under critical cornering involved a fatigue sensitivity analysis for the given loads. Form Figure 9(b), it was identified that for the critical cornering loading conditions, the suspension system was operating within the limit of infinite life for all components.

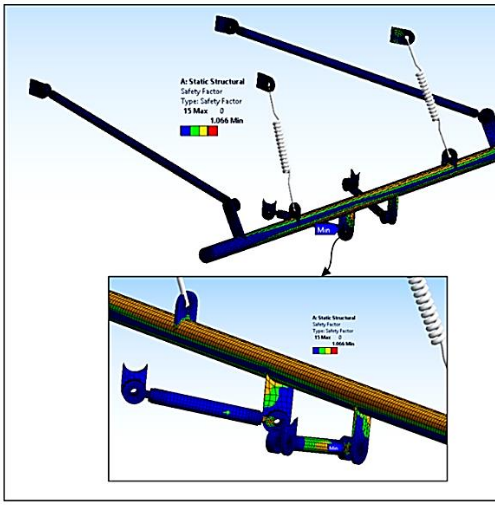

(a)

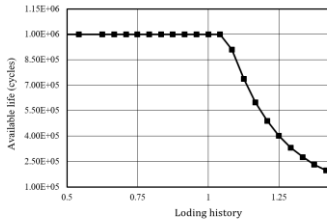

(b)

Figure 9 (a) Safety factor for critical cornering load, (b) Fatigue sensitivity graph

Through the design iterations, the mounting brackets on the beam axle and frame have been considerably angled. This ensures that the rod ends are not misaligned at a static position, but rather directly link the frame and the rear axle. This rotation of the brackets also ensures there is 12 degrees of allowable misalignment in the spherical bearing of the heim joint. This allows effective movement of the suspension system and prevents clashing of components during dynamic loads and suspension travel. Using ANSYS, the critical bolted joint was found to be withstand the forces applied while under critical loading. The M10x50 mm grade 8.8 high tensile bolt was analyzed with a 21.9 kN pretension to suit an assembly torque of 44Nm. The performance of the bolt and joint can be seen in Figure 10. The maximum stress on the bolt is 57.16 MPa which is significantly below the yield strength of the bolt which is 640 MPa.

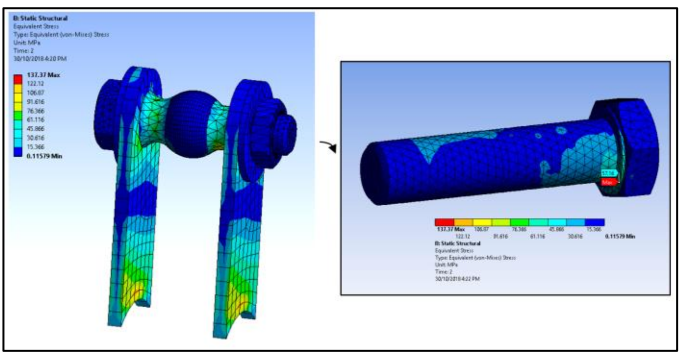

Figure 10 Bolt performance

5 CONCLUSION

This paper provides key considerations for designing and analyzing rear suspension system of a Formula SAE vehicle produced by James Cook University students. They were addressed appropriately because of the successful performance of the designed vehicle during driver's training and at the 2019 Formula SAE competition. With the proposed suspension which is a dependent one and based on the finite element analysis, the stress concentration of the proposed design is significantly low under different load cases. The dependent system transfers the load transmitted through the larger beam axle and consequently has a lower maximum stress. It is shown that since the beam axle is mounted to the upright by means of the weld-in bung, the contact surface area for the transmitted forces is significantly large. This ultimately leads to lower stress values present resulting in a higher safety factor. Utilizing a material with a high strength to weight ratio, Chromoly, allows the overall size of the beam axle to be reduced to avoid clashes with components. With the implementation of Chromoly as a substitute for mild steel and thicker material utilized, the safety factor and life cycle are significant high; under considered load conditions the proposed suspension system would operate for infinite life. With the trailing arms angled in the design of the suspension geometry, the undesirable bending within the trailing arms is avoided and a reduction in stress and higher roll center are provided. Moreover, it is proposed that the stress concentration in brackets with filleted corner is considerably lower than those with sharp corners, which means better stress distribution in the component and consequently higher life cycle for the whole system.

APPENDIX A

Forces acting on the rear suspension for linear acceleration load case:

$$\text{longitudinal weight transfer} = \frac{\text{acceleration}\times\text{COM height}\times\text{weight}}{2\times\text{wheelbase}} = 42.94\ \text{kg}$$

$$\text{vertical weight transfer} = \text{weight transfer} + \text{weight distribution} = 42.98\times 9.81 + 1107 = 1528.28\ \text{N}$$

$$\text{friction force} = \text{vertical force}\times\text{friction coefficient} = 1528.25\times 0.8 + 1107 = 1222.4\ \text{N}$$

Forces acting on the rear suspension for braking load case:

$$\text{longitudinal weight transfer} = \frac{\text{acceleration}\times\text{COM height}\times\text{weight}}{2\times\text{wheelbase}} = 42.94\ \text{kg}$$

$$\text{vertical weight transfer} = \text{weight transfer} + \text{weight distribution} = 1107 - 42.94\times 9.81 = 658.76\ \text{N}$$

$$\text{friction force} = \text{vertical force}\times\text{friction coefficient} = 658.76\times 0.8 = 548.61\ \text{N}$$

APPENDIX B

Endurance limit modifying factor for fatigue analysis:

$$endurance\ limit\ factor = k_a k_b k_c k_d k_e k_f$$

$k_a: surface\ modification\ factor$ $\quad k_a = a\times S_{ut}^{b} = 4.51\times 460^{-0.265} = 0.888$

$k_b: size\ factor$ $\quad k_b = 1.24(0.37\times d)^{-0.107} = 1.04$

$k_c: loading\ factor$ $\quad k_c = 1$

$k_d: temperature\ factor$ $k_d = 1$ (temperature is below 400℃)

$k_e: reliabity\ factor$ $k_e = 0.753$ (reliability is assumed to be 99.9%)

$k_e: miscellaneous\ effect\ factor$ $k_f = 1$

$$\rightarrow\ endurance\ limit\ factor = 0.67$$

REFERENCES

[1] Formula SAE Rules 2018, Available: https://www.fsaeonline.com/content/201718%20FSAE%20Rules%209.2.16a.pdf.

[2] S.D. Shinde, S. Maheshwari, S. Kumar, Literature review on analysis of various Components of McPherson suspension, Materials Today: Proceedings, 5 (2018).

[3] S. Khan, Y. Joshi, A. Kumar, R.B. Vemuluri, Comparative study between double wish-bone and macpherson suspension system, IOP Conference Series: Materials Science and Engineering, 263 (2017) 062079.

[4] D. Kazmirowicz, Design and Investigation of a Lightweight Formula-SAE, in, School of Mechanical Engineering, University of Western Australia, 2004.

[5] M. Kiszko, REV 2011 Formula SAE Electric in, School of Mechanical Engineering, University of Western Australia, 2011.

[6] A.C. Cobi, Design of a Carbon Fiber Suspension System for FSAE Applications, in, Deptartment of Mechanical Engineering, Massachusetts Institute of Technology, 2012.

[7] M. McCune, D. Nunes, M. Patton, C. Richardson, E. Sparer, Formula SAE Interchangeable Independent Rear Suspension Design, California Polytechnic State University, California, (2009).

[8] C. Smith, Tune To Win, Aero Publishers, 1978.

[9] R.K. Rathore, E.N. Karlus, R.L. Himte, Weight Optimization of Mono Parabolic Leaf Spring, International Journal of Advances in Engineering & Technology, 3 (2014).

[10] J.M. Wong, Solid axle suspension for vehicles in: General Motors Corporation, 1998.

[11] R. Bolig, Art Morrison Enterprises Talks About Rear Suspensions, Available at: https://www.chevyhardcore.com/news/suspension-art-morrison/, 2018.

[12] D.I.H. Parkin, Design of a rear suspension configuration for a live axle race car to achieve optimum handling characteristics, in, Faculty of Engineering and Surveying, University of Southern Queensland, 2007.

[13] L. Plumb, The design, manufacture, and analysis of a competition chassis for the JCU FSAE car, in, School of Mechanical Engineering, James Cook University, 2014.

[14] L.V. Fornace, Weight Reduction Techniques Applied to Formula SAE Vehicle Design: An Investigation in Topology Optimization, in, University of California, 2006.

[15] J. Dombrose, B. Hendry, Stability and on-road performance of multi-combination vehicles with air suspension systems project, in, Department for Planning and Infrastructure Roaduser Systems Pty Ltd, 2005.

[16] R. Budynas, K. Nisbett, Shigley's Mechanical Engineering Design, McGraw-Hill Series in Mechanical Engineering, 2006.

MOBILITY & VEHICLE MECHANICS

DOI:10.24874/mvm.2020.46.02.02
UDC: 629.021

DESIGN AND ANALYSIS OF SINGLE PLATE CLUTCH USING ANSYS

Kedar Kishor Patil[1], *Vinit Randiv*[2], *Sahil Mulla*[3], *Rajkumar Parit*[4], *Sagar Mane*[5], *Sunil Kadam*[6]

Received in June 2020 Accepted in August 2020

RESEARCH ARTICLE

ABSTRACT: This paper addresses modelling and analysis of single plate clutch which is used in Tata Sumo vehicle. Clutch is the most significant component located between engine and gear box in automobiles. The static and dynamic analysis were developed for a clutch plate by using finite element analysis (FEA). The 3D solid model was done using CATIA V5R16 version and imported to ANSYS work bench 19.0 for structural, thermal and modal analysis. The mathematical modelling was also done using six different materials (i.e. Steel, Stainless Steel, Ceramics, Kevlar, Aluminium alloy and Gray Cast iron); then, by observing the results, comparison was carryout for materials to validate better lining material for single plate clutches using ANSYS workbench 19.0 and finally conclusion was made.

KEY WORDS: Modeling single plate clutch using CATIA, Analysis of single plate clutch using ANSYS, Clutch materials, Tata Sumo

[1] Kedar Kishor Patil, *Bharati Vidyapeeth's College of Engineering Kolhapur, Maharashtra, India*, *kedarkishorpatil@gmail.com*, *(*corresponding author)*
[2] Vinit Randiv, *Bharati Vidyapeeth's College of Engineering Kolhapur, Maharashtra, India*
[3] Sahil Mulla, *Bharati Vidyapeeth's College of Engineering Kolhapur, Maharashtra, India*
[4] Rajkumar Parit, *Bharati Vidyapeeth's College of Engineering Kolhapur, Maharashtra, India*
[5] Sagar Mane, *Bharati Vidyapeeth's College of Engineering Kolhapur, Maharashtra, India*
[6] Sunil Kadam, *Bharati Vidyapeeth's College of Engineering Kolhapur, Maharashtra, India*

DIZAJN I ANALIZA PRENOSNE PLOČE JEDNOSTRUKE SPOJNICE PRIMENOM ANSIS-A

REZIME: Ovaj rad se bavi modeliranjem i analizom jednostruke spojnice koja se koristi u vozilu Tata Sumo. Spojnica je najznačajnija komponenta koja se nalazi između motora i menjača u automobilima. Statička i dinamička analiza razvijene su za prenosnu ploču spojnice primenom analize konačnih elemenata (FEA). Prostorni 3D model urađen je pomoću programskog paketa CATIA V5R16 i uvezen u programski paket ANSIS 19.0 za strukturnu, termičku i modalnu analizu. Matematičko modeliranje je urađeno za šest različitih materijala (nerđajući čelik, keramika, kevlar, legura aluminijuma i sivi liv). Analizom rezultata, upoređeni su materijali da bi se izabrao bolji materijal prenosne ploče jednostruke spojnice pomoću ANSIS-a 19.0.

KLJUČNE REČI: hidraulična transmisija, osnosimetrično strujanje, razmena energije, projektovanje, lopatica

DESIGN AND ANALYSIS OF SINGLE PLATE CLUTCH USING ANSYS

Kedar Kishor Patil, Vinit Randiv, Sahil Mulla, Rajkumar Parit, Sagar Mane, Sunil Kadam

1. INTRODUCTION

A Clutch is the first element of power train used on the transmission shafts. The main function of clutch is to engage and disengage the engine to transmission, when the driver needs or during shifting of gear. When the clutch is in engaged position, the power flows from the engine to the wheel and when it is in disengage position, the power is not transmitted to the wheel. In automobile, a gearbox is required to change the speed and torque of the vehicle. If we change a gear, when the engine is engaged with gearbox or when the gears are in running position then it can cause of wear and tear of gears. To overcome this problem a clutch is used between gearbox and engine. Some friction plates, sometimes known as clutch plates are kept between these two members. The clutch is based on the friction. When two friction surfaces brought in contact and pressed, then they are united due to friction force between them. The friction between these two surfaces depends on the area of surface, pressure applied upon them and the friction material between them. The driving member of a clutch is the flywheel mounted on the engine crankshaft and the driven member is pressure plate mounted driving shaft to the driven shaft so that the driven shaft may be started or stopped at will, without stopping the driving.

The two main types of clutch are: positive clutch and friction clutch. Positive clutches are used when positive drive is required. The simplest type of a positive clutch is a jaw or claw clutch. A friction clutch has its principal application in the transmission of power of shafts and machines which must be started and stopped frequently. The force of friction is used to start the driven shaft from rest and gradually brings it up to the proper speed without excessive slipping of the friction surfaces. In automobiles, friction clutch is used to connect the engine to the drive shaft. The primary aim of this work is to design a rigid drive clutch system that meets multiple objectives such as Structural strength.

Gradual engagement clutches like the friction clutches are widely used in automotive applications for the transmission of torque from the flywheel to the transmission. The three major components of a clutch system are the clutch disc, the flywheel and the pressure plate. Flywheel is directly connected to the engine's crankshaft and hence rotates at the engine rpm. Bolted to the clutch flywheel is the second major component: the clutch pressure plate. The spring-loaded pressure plate has two jobs: to hold the clutch assembly together and to release tension that allows the assembly to rotate freely. Between the flywheel and the pressure plate is the clutch disc. The clutch disc has friction surfaces similar to a brake pad on both sides that make or break contact with the metal flywheel and pressure plate surfaces, allowing for smooth engagement and disengagement.

In short in an automobile clutch is need for Torque transmission; Gradual Engagement; Heat Dissipation; Dynamic Balancing; Vibration Damping; Size; Inertia and Ease of operation of vehicle.

2. SELECTION OF MATERIAL

The following materials used for Friction clutch plate:

2.2.1. Gray cast iron as Friction material: Gray has a graphitic microstructure. The clutch disc is generally made from grey cast iron this is because it has a good wear resistance with high thermal conductivity and the production cost is low compare to other clutch disc materials.

2.2.2. Kevlar 49 as friction material: Kevlar was introduced by DuPont in the 1970s. It was the first organic fiber with sufficient tensile strength and modulus to be used in advanced composites. Originally developed as a replacement for steel in radial tires, Kevlar is now used in a wide range of applications.
2.2.3 Ceramic as friction material: Ceramic clutch plates are, ironically, made with a combination of copper, iron, bronze, and silicon and graphite. Because of their metallic content, these discs can withstand a lot of friction and heat. This makes them ideal for race cars and other high-speed vehicles that need to engage and disengage from fast-moving flywheels.
2.2.4 Aluminum alloy as friction material: The unique properties of aluminum composites are better comparing to other conventional materials. Aluminum composites can use because of its strong bonding, good corrosion resistance, good wet ability, low density and high flexibility.
2.2.5 Steel as friction material: Steel is the primary mating surface used in clutches and can be used as the primary heat sink or the means to dissipate the energy into the ambient surroundings. In a "wet" or oil-immersed application, oil molecules are trapped between the steel mating plate and the friction material. The surface roughness of the steel mating plate and the texture of the friction material combine on shear of the oil to deliver a co-efficient of friction of up to 0.15. However, these discs are high-friction. This means that the engagement and disengagement of the clutch won't always be very smooth.

Table 1. Comparison of materials based on its Mechanical property

Sr. No.	**Material**	**Specific Strength *(kN-m/kg)***	**Yield Strength (Mpa)**	**Elastic Modulus (Gpa)**	**Friction coefficient**	**Density [kg/m^3]**
1	Steel	46	420	210	0.42	7861
2	Stainless Steel	65	505	195	0.57	7610
3	Ceramics	6.7	457	33	0.4	3500
4	Kevlar 49	23.8	370	72	0.5	1470
5	Aluminum alloy 6061	4.5	275	69.7	0.23	2700
6	Gray Cast iron	19.1	720	24.1	0.28	7200

3. CALCULATIONS

Clutch plate of a TATA SUMO was selected for analysis.

Table 2. Specifications of Tata Sumo vehicle

Parameter	**Value**
Torque (T)	300 N-m at 1000 rpm
Outer Radius of Friction Face (R_o)	160 mm
Inner Radius of Friction Face (R_i)	90 mm
Maximum Power	64 KW at 3000 rpm
Maximum Pressure Intensity (P)	0.5N/mm^2

Torque transmission under uniform pressure: This theory applies to new clutch. In new clutches the pressure can be assumed as uniformly distributed over the entire surface area of the friction disk. With this assumption, the intensity of pressure between disks, is regarded as constant.

Torque transmission under uniform wear: This theory is based on the fact that the wear is distributed uniformly across the entire friction disk surface area. This assumption can be used for worn out clutches or old clutches. The axial wear of the friction disk is proportional to frictional work. The work done by the friction is proportional to the frictional force and the rubbing velocity. The uniform-pressure theory is applicable only when the friction lining is new. When the friction lining is used over a period of time, wear occurs. Therefore, the major portion of the life of friction lining comes under uniform-wear criterion. Hence, in the design of clutches, the uniform wear theory is used.

Uniform Pressure Theory	**Uniform Wear Theory**
$P = \frac{F}{\pi(R_o^2 - R_i^2)}$	$P = \frac{F}{2\pi r(R_o - R_i)}$ Where Pr=constant
$T = \mu F \frac{2}{3}\frac{(R_o^3 - R_i^3)}{(R_o^2 - R_i^2)}$	$T = \mu F \frac{1}{2}(R_o + R_i)$

Where,
P=normal pressure
F=axial force
μ=coefficient of friction between the surfaces
T=friction torque

R_o = outer radius
R_i = inner radius

Calculation for the friction lining based on uniform wear theory and Uniform pressure theory:

Effective mean radius **r** for uniform wear theory = $\frac{Ri+Ro}{2} = \frac{90+160}{2}$ = 125 mm

Effective mean radius **r** Uniform pressure theory = $\frac{2(R_0^3-R_i^3)}{3(R_0^2-R_i^2)} = \frac{(2*160*160*160)-(2*90*90*90)}{(3*160*160)-(3*90*90)}$ = 128.6 mm

Area of friction pads (A) = π (R_o^2-R_i^2) = π (160^2-90^2) = 54977.87 mm^2

Angular velocity (ω) =2πN/60 = (2π*3000)/60 = 314.16 rad/sec.

Heat generation in watts (Q_g) = Coefficient of friction * Maximum Pressure *Angular velocity

= μ*Pmax*ω

Heat flux obtained in clutch plate (Q_f) = heat generated in clutch plate/surface area = Qg/A

Table 3. Results for uniform wear and uniform pressure theory

Sr. No.	**Materials**	**Coefficient of friction [μ]**	**Uniform pressure**		**Uniform wear**		**Heat Flux (Q_F) (Watt/mm²)**
			Axial force [N]	**Pressure [N/mm²]**	**Axial force [N]**	**Pressure [N/mm²]**	
1.	Steel	0.16	14580	0.27	15000	0.27	$4.57*10^{-4}$
2.	Stainless Steel	0.15	15552	0.29	16000	0.29	$4.28*10^{-4}$
3.	Ceramics	0.6	03888	0.07	04000	0.07	$1.71*10^{-3}$
4.	Kevlar	0.5	04665	0.09	04800	0.08	$1.42*10^{-3}$
5.	Aluminum alloy	0.23	10142	0.19	10435	0.18	$6.57*10^{-4}$
6.	Gray Cast iron	0.28	08332	0.15	08571	0.16	$08.0*10^{-4}$

4. FEA ANALYSIS

Finite element analysis is the computational tool most widely accepted in engineering analysis. The clutch plate assembly is modelled in CATIA software imported to ANSYS to do static structural analysis, thermal analysis and modal analysis. Using different lining materials finite element analysis has been done.

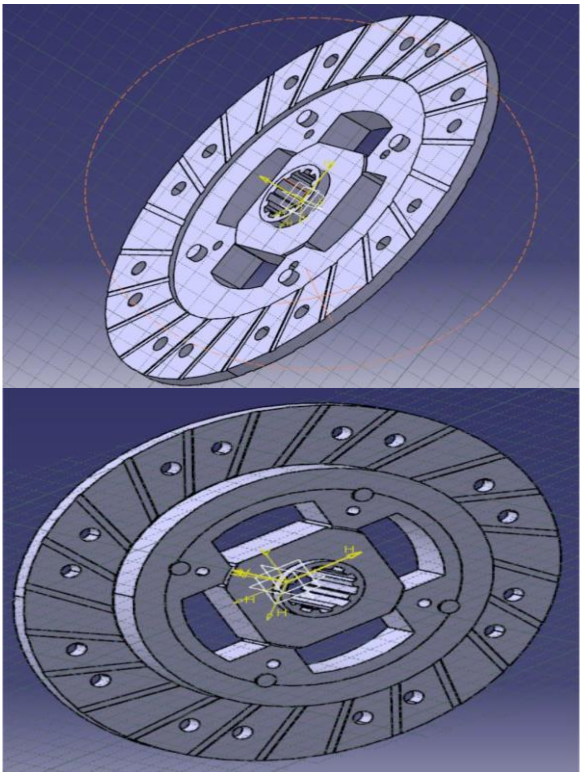

Figure 1. CATIA model of Tata Sumo clutch plate

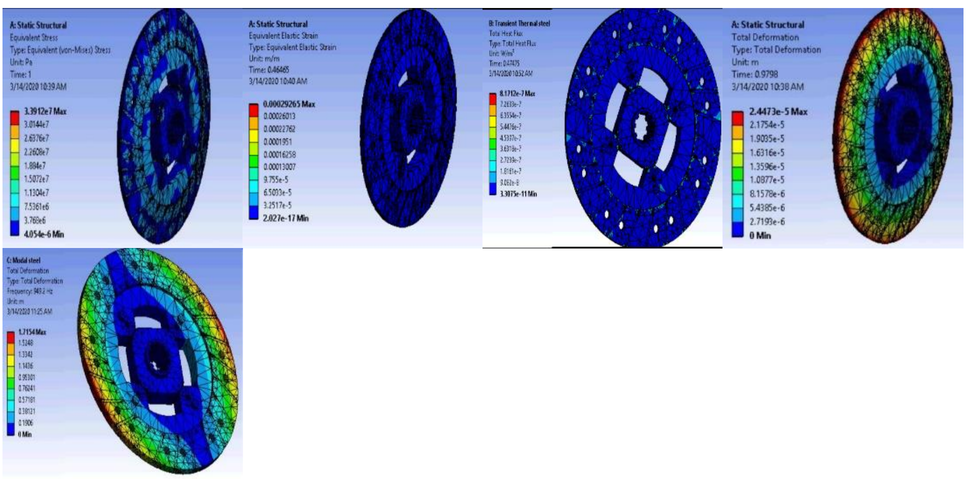

(A) ***(B)*** ***(C)*** ***(D)***

(i)

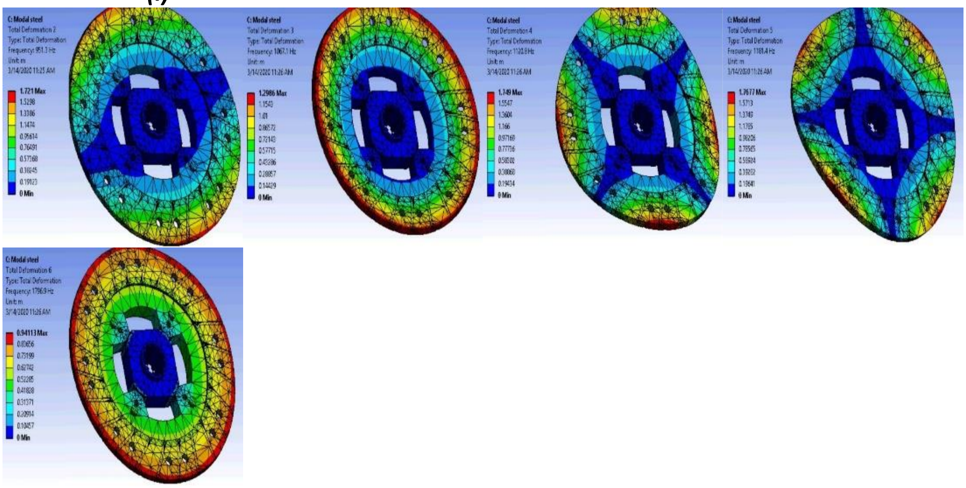

(ii) ***(iii)*** ***(iv)*** ***(v)***

(vi)

*Figure 2. Structural Steel as friction material as friction material **(A)** Von-Mises Stress; **(B)** Von-Mises Strain; **(C)** Total Heat Flux;**(D)** Total Deformation; **(i to vi)** first six modal frequencies*

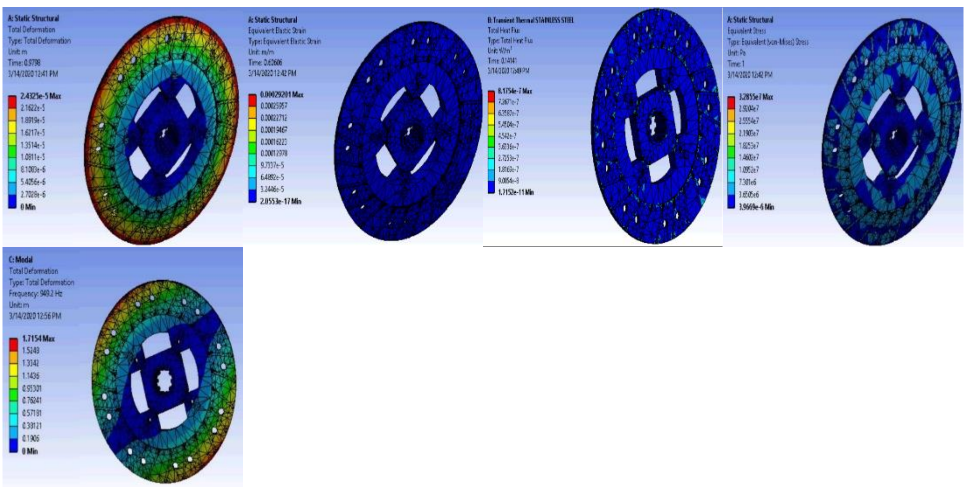

(A) ***(B)*** ***(C)*** ***(D)***

(i)

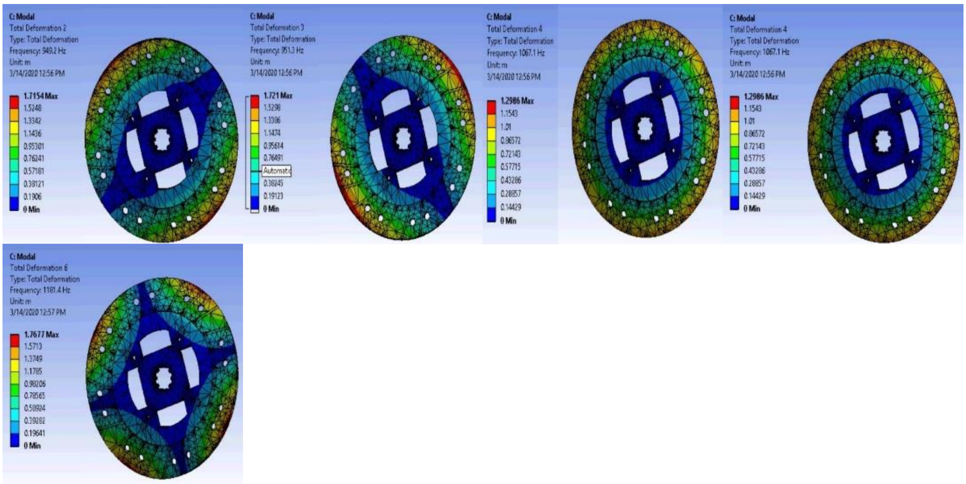

(ii) (iii) (iv) (v) (vi)

*Figure 3. Stainless Steel as friction material **(A)** Von-Mises Stress; **(B)** Von-Mises Strain; **(C)** Total Heat Flux; **(D)** Total Deformation; **(i to vi)** first six modal frequencies*

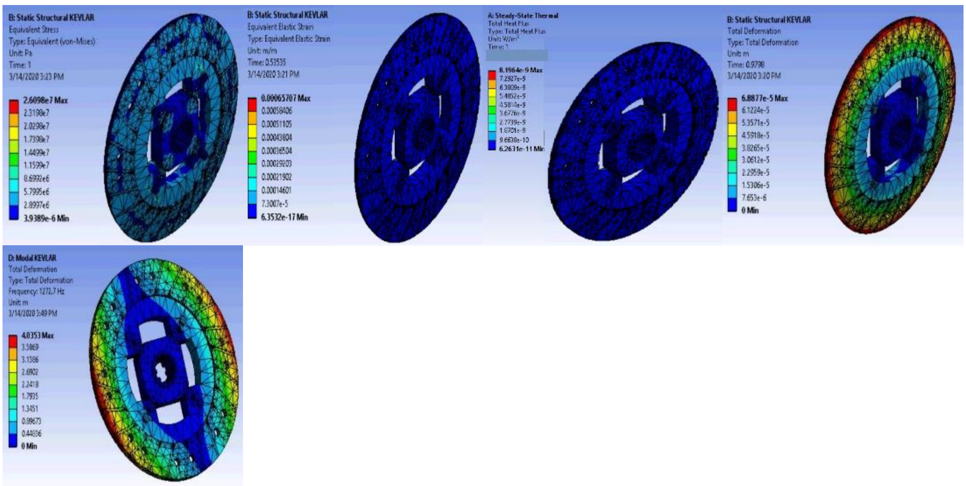

(A) (B) (C) (D) (i)

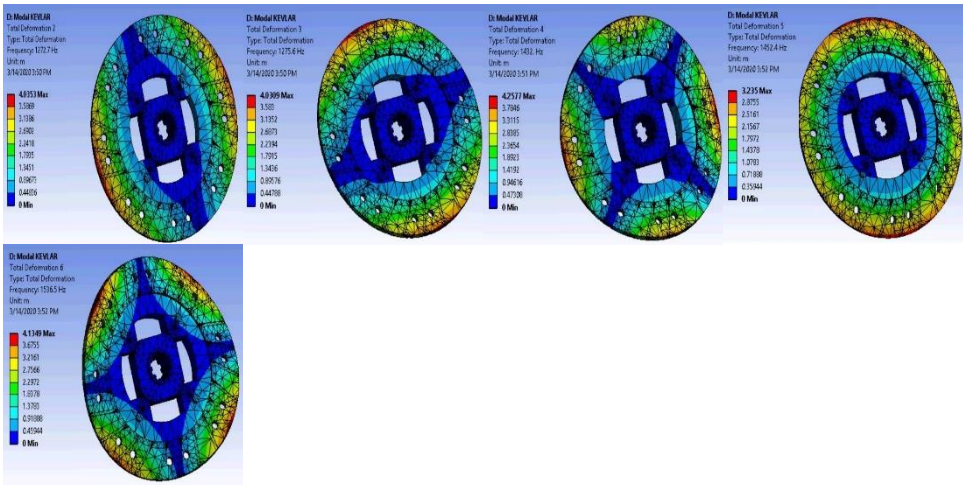

(ii) ***(iii)*** ***(iv)*** ***(v)*** ***(vi)***

Figure 4. Kevlar 49 as friction material ***(A)*** *Von-Mises Stress;* ***(B)*** *Von-Mises Strain;* ***(C)*** *Total Heat Flux;* ***(D)*** *Total Deformation;* ***(i to vi)*** *first six modal frequencies*

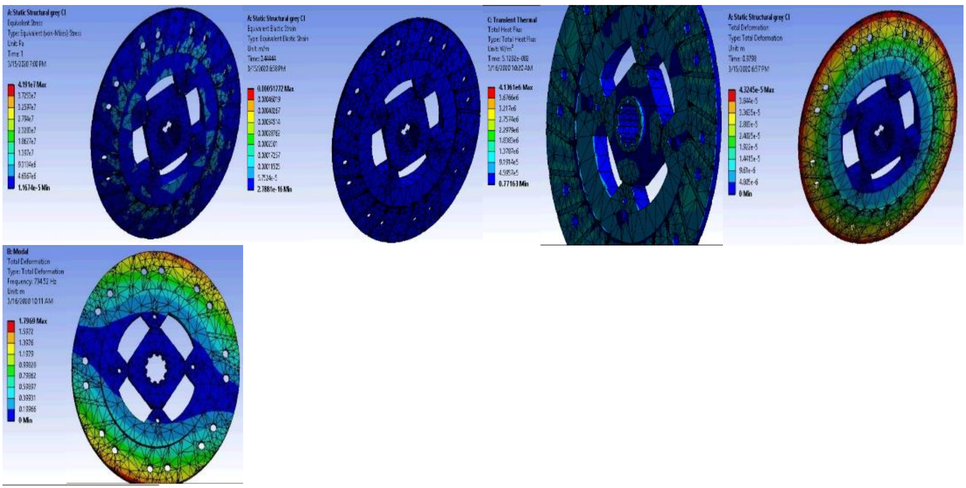

(A) ***(B)*** ***(C)*** ***(D)*** ***(i)***

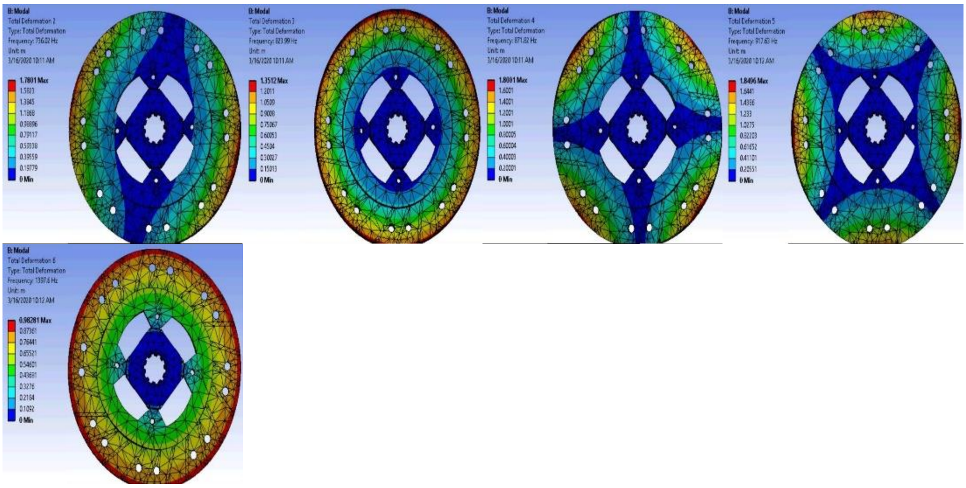

(ii) (iii) (iv) (v) (vi)

*Figure 5. Grey Cast Iron as friction material **(A)** Von-Mises Stress; **(B)** Von-Mises Strain; **(C)** Total Heat Flux; **(D)** Total Deformation; **(i to vi)** first six modal frequencies*

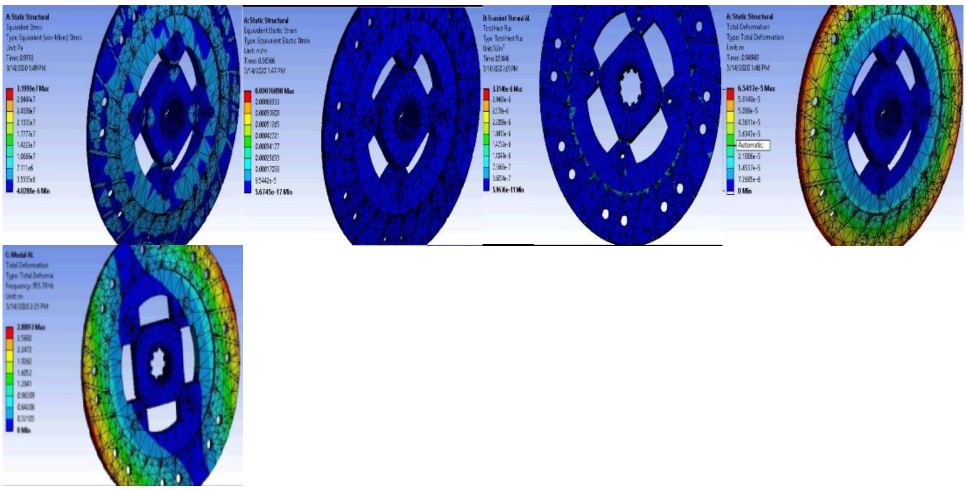

(A) (B) (C) (D) (i)

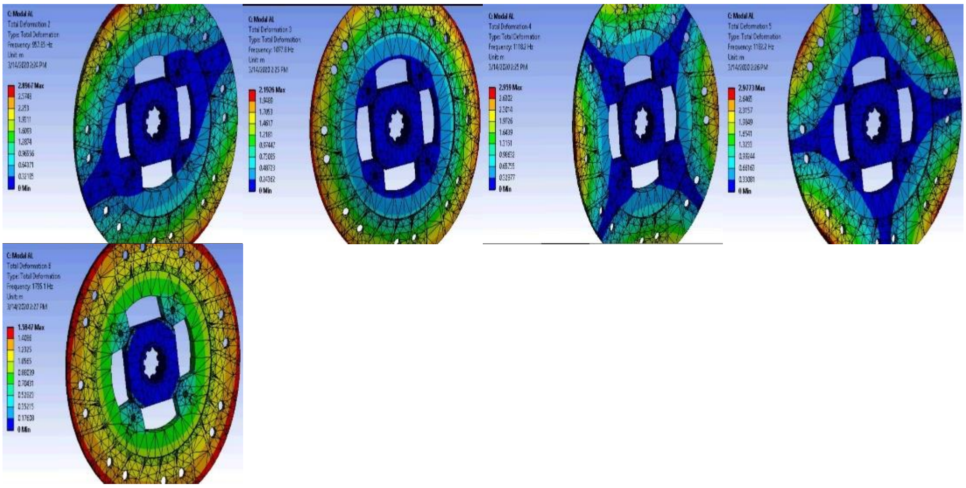

(ii) ***(iii)*** ***(iv)*** ***(v)*** ***(vi)***

*Figure 6. Aluminum alloy as friction material as friction material **(A)** Von-Mises Stress; **(B)** Von-Mises Strain; **(C)** Total Heat Flux; **(D)** Total Deformation; **(i to vi)** first six modal frequencies*

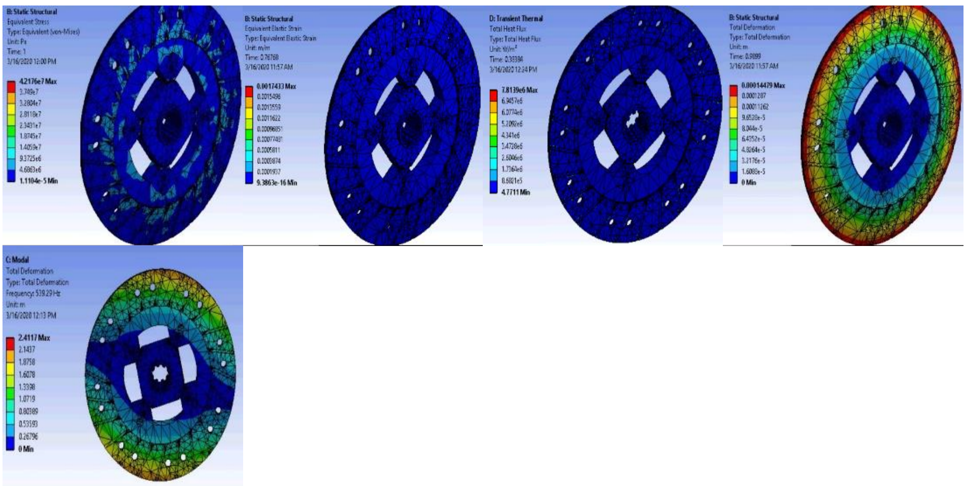

(A) ***(B)*** ***(C)*** ***(D)*** ***(i)***

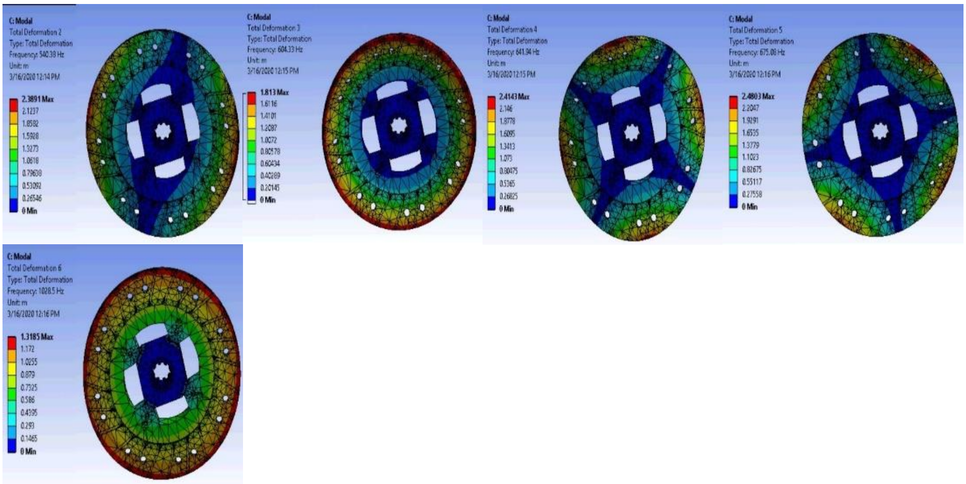

(ii) (iii) (iv) (v) (vi)

*Figure 7. Ceramic as friction material **(A)** Von-Mises Stress; **(B)** Von-Mises Strain; **(C)** Total Heat Flux; **(D)** Total Deformation; **(i to vi)** first six modal frequencies*

Table 4. Results for Structural Analysis in ANSYS

Sr. No.	**Materials**	**Total Deformation [m]**	**Von mises Equivalent Stress [Pa]**	**Von mises Equivalent Strain**	**Total Heat Flux [W/m^2]**	**Poisson's Ratio**	**Youngs Modulus [Pa]**
1.	Structural Steel	$2.4473*10^{-5}$	$3.3912*10^{7}$	$2.926*10^{-4}$	$8.17*10^{-7}$	0.3	$2.00*10^{11}$
2.	Structural Steel	$2.4473*10^{-5}$	$3.2855*10^{7}$	$2.920*10^{-4}$	$8.17*10^{-7}$	0.31	$1.93*10^{11}$
3.	Kevlar 49	$6.8877*10^{-5}$	$2.6098*10^{7}$	$6.570*10^{-4}$	$8.18*10^{-9}$	0.44	$6.20*10^{10}$
4.	Gary Cast Iron	$4.3245*10^{-5}$	$4.1913*10^{7}$	$5.177*10^{-4}$	$4.13*10^{6}$	0.28	$1.10*10^{11}$
5.	Aluminum Alloy	$6.5417*10^{-5}$	$3.1999*10^{7}$	$7.689*10^{-4}$	$3.31*10^{-6}$	0.33	$7.10*10^{10}$
6.	Ceramic	$1.4794*10^{-5}$	$4.2176*10^{7}$	$1.740*10^{-4}$	$7.81*10^{6}$	0.27	$4.10*10^{11}$

Table 5. Results for Natural Frequencies obtained from Modal Analysis in ANSYS

First Six Modal Frequencies in Hz	**Materials**					
	Structural Steel	**Structural Stainless Steel**	**Kevlar 49**	**Gary Cast Iron**	**Aluminium Alloy 6061**	**Ceramic**
1.	949.2	949.2	1272.7	734.52	955.1	539.29
2.	951.3	951.3	1275.6	736.02	957.8	540.38

3.	1067.1	1067.1	1432	823.99	1077.8	604.33
4.	1120.8	1120.8	1452.4	871.82	1118.2	641.94
5.	1181.4	1181.4	1536.5	917.63	1182.2	675.08
6.	1796.9	1796.9	2302.3	1397.6	1785.1	1028.5

5. CONCLUSION

In this work, clutch plate of Tata Sumo has been designed. Clutch plate has been modelled in CATIA software and simulated using ANSYS software for different materials. Effect of same pressure intensity of 0.5N/mm^2 for different materials has observed. Heat flux, Total deformation, stress, strain and first six modal frequencies for different materials are observed. By comparing the results tabulated in table 4 it is clear that ceramic has less deformation and less modal frequencies than all other. This data helps the researchers to select proper material to reduce wear and increase life of clutch.

REFERENCES

[1] Narayan S., Effects of Various Parameters on Piston Secondary Motion, SAE Technical Papers, 2015, 2015-01-0079, doi: https://doi.org/10.4271/2015-01-0079.

[2] Mrs.Ch.Vasantha Lakshmi, and SandhyaRani.V, Design and Structural Analysis of Composite Coated Clutch Plate by using Composite Materials, International Journal and Magazine of Engineering, Technology, Management and Research, A peer Reviewed Open Access International Journal. ISSN No: 2348-4845. P1-4, (retrived on, Dec. 12,2016)

[3] A&C Automotive, Internet address: http://www.acautomotive1.co.uk/clutches.php, accessed 10.03.2018.

[4] Narayan S., A review of diesel engine acoustics, FME Transactions, 2014, 42(2), 150-154, doi: 10.5937/fmet1402150N.

[5] Mamata G. Pawar, Monarch K. Waramble, Gautam R. Jodh, Design and Analysis of clutch using Sintered iron as a Friction material, International Journal of Innovative Technology and Exploring Engineering. December 2013.

[6] P. Naga Karna, Tippa Bhimasankhara Rao, Analysis of Friction clutch plate using FEA, International Journal of Engineering Research and Development, Vijayawada, March 2013.

MOBILITY & VEHICLE MECHANICS

DOI:10.24874/mvm.2020.46.02.03
UDC: 629.33;658.138

LOGISTICS OF ELECTRIC DRIVE MOTOR VEHICLES RECYCLING

Saša Milojević[1], Ivan Miletić[2], Blaža Stojanović[3], Ivana Milojević[4], Marko Miletić[5]

Received in August 2020 Revised in September 2020 Accepted in September 2020

RESEARCH ARTICLE

ABSTRACT: Increase in number of transport vehicles, especially motor vehicles, has negative impact on environment. It refers to air pollution problem due to usage (combustion) of fossil fuels in motor vehicles. Agriculture activities, factories, industry and many other activities additionally contributes to air pollution. Greenhouse gas emission is main cause of global warming and air pollution, and mainly occurs due to industry and transport.

In many countries, the adoption of legislation gives priority to the use of electric vehicles due to lower emissions compared to conventionally powered vehicles (diesel or gasoline engines). In this way, goals have been set in the European Union and regulations have been passed which, among other things, require a certain percentage of motor vehicle recycling at the end of their service life. The Directive 2000/53/EC of the European Parliament and of the Council regulates waste management in the vehicle sector.

Due to the increased number of electric vehicles, which participate in the transport of goods and people, the paper partially analyzes the problem related to the adaptation of existing recycling centers (for classic vehicles), for the needs of recycling electric vehicles and their specific parts and equipment (such as magnets and electric motors).

KEY WORDS: Electric drive, motor vehicles, recycling

[1] *Saša Milojević, expert advisor, University of Kragujevac, Faculty of Engineering, e.mail: sasa.milojevic@kg.ac.rs, (*corresponding author)*
[2] *Ivan Miletić, assist. prof., University of Kragujevac, Faculty of Engineering*
[3] *Blaža Stojanović, prof., University of Kragujevac, Faculty of Engineering*
[4] *Ivana Milojević, MSc student, University of Kragujevac, Faculty of Engineering*
[5] *Marko Miletić, University of Kragujevac, Faculty of Engineering*

LOGISTIKA RECIKLAŽE MOTORNIH VOZILA NA ELEKTRIČNI POGON

REZIME: Povećanje broja transportnih sredstava, prvenstveno motornih vozila, ima negativan uticaj na čovekovu okolinu. To se odnosi na problem zagađenja vazduha zbog upotrebe (sagorevanja) goriva fosilnog porekla u motornim vozilima. Zagađenju vazduha dodatno doprinose aktivnosti na poljoprivredi, fabrike i industrija i mnoge druge aktivnosti. Emisija gasova staklene bašte je glavni uzročnik globalnog zagrevanja i zagađenja vazduha i nastaje uglavnom zbog industrijske ativnosti i transporta.

U mnogim državama se donošenjem zakonskih propisa daje prioritet upotrebi vozila na električni pogon zbog manje emisije u odnosu na vozila sa klasičnim pogonom (dizel ili benzinskim motorima). Tim putem su u Evropskoj uniji postavljeni ciljevi i donešeni su propisi kojima se između ostalog zahteva određeni procenat reciklaže motornih vozila na kraju njihovog servisnog veka. Direktivom Evropskog parlamenta i Saveta (engl. Directive of the European Parliament and of the Council 2000/53/EC) uređuje se upravljanje otpadom u sektoru vozila.

Zbog sve većeg broja vozila na električni pogon, koja učestvuju u transportu robe i ljudstva, u okviru rada je delom analiziran problem koji se odnosi na adaptaciju postojećih reciklažnih centara (za klasična vozila), za potrebe reciklaže vozila na električni pogon i njihovih specifičnih delova i opreme (kao što su magneti i električni motori).

KLJUČNE REČI: Električni pogon, motorna vozila, reciklaža

LOGISTICS OF ELECTRIC DRIVE MOTOR VEHICLES RECYCLING

Saša Milojević, Ivan Miletić, Blaža Stojanović, Ivana Milojević, Marko Miletić

1. INTRODUCTION - ENVIRONMENTAL PROTECTION AND RECYCLING OF MOTOR VEHICLES - CONDITION AND LEGAL REGULATIONS

One of the basic goals is protection of the environment. The importance of this goal can be illustrated by data related to the production of motor vehicles.

It is estimated that approximately 107 million vehicles will be produced worldwide by the end of 2020. A total of about 79 million cars are expected to be sold worldwide. By comparison, over 26 million motor vehicles were sold worldwide in 2017, with U.S. the largest market for commercial vehicles (trucks and buses) [1, 2].

The transport sector is responsible for one quarter of the total greenhouse gas emissions in the European Union (EU). The largest emission is generated by the energy sector, followed by transport, industry, households, agriculture, etc., Figure 1 [3].

Road traffic emits a fifth of the total carbon dioxide (CO2) emissions in the EU that is more than two thirds of the total greenhouse gas emissions emitted by vehicles during various modes of transport [1, 2].

The rest of this paper is organized as follows. In Section 2, independent and dependent suspension systems are introduced. Preliminary considerations, including design constraints and load conditions, and design development are proposed in section 3. Numerical analysis of the proposed system is presented in Section 4. Finally, in Section 5, conclusions are presented.

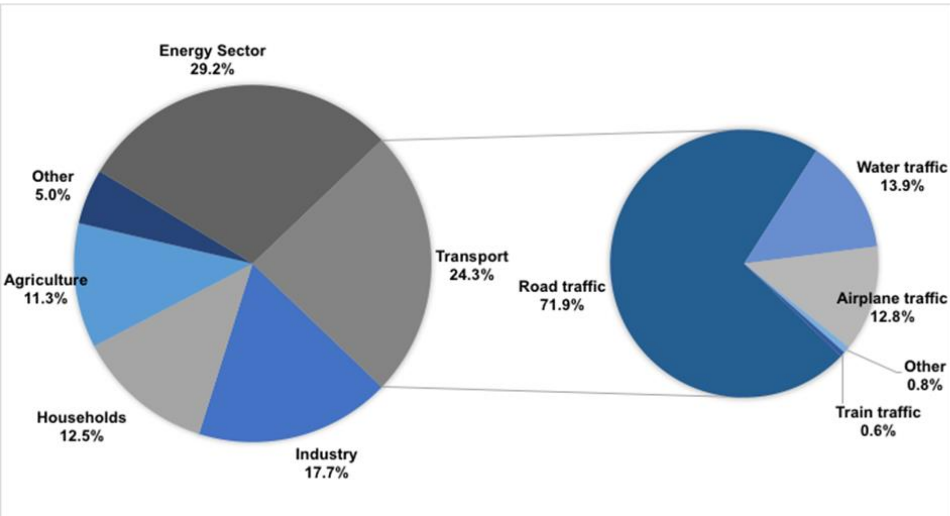

Figure 1: *(EU28) Greenhouse gas emissions by sectors and presentation of the share of road traffic*

Due to the increasing load on the environment with the increase in the number of motor vehicles in use, the emission of noise and toxic exhaust gases has increased, which must be limited and reduced. Also, a large amount of materials, different types of metals and fluids are used within the vehicle, which have to be produced from renewable raw materials and which must be recycled [4-6].

In this way, the 20/20/20 strategy was implemented in the European Union, which was established in 2007 and included the following three goals: increase of energy efficiency by 20%, reduction of carbon dioxide emissions by 20% and 20% share of renewable energy sources, for period until 2020. In general, the goal is to reduce carbon dioxide emissions by 40% by 2030, if we look at the value of emissions from 1990 that is to reduce emissions by 80-95% by 2050 [1, 2].

Due to all the above, electric drive is a serious alternative to classic motor vehicle drive systems. As an example, the number of cars with exclusively electric drive between 2017 and 2018 increased by 43% in the EU. More than one million electric (plug-in) passenger and light cargo (truck vans) vehicles were registered by the beginning of June 2018 in Europe. Mass registration of such vehicles has been recorded only in China [3, 7].

In general, parallel in the world, in addition to the classic ones, the number of written-off electric vehicles, which are at the end of the service life (ELV) and which must also be recycled, is increasing. Therefore, it is important to introduce certain regulations in this area. It is also important to reduce the illegal sale of written-off vehicles, instead of recycling them, and to strengthen inspections in this area inside and outside the EU.

Appropriate regulations must regulate the procedures from writing off the vehicle to disassembling the vehicle into its component parts, their classification, recycling and re-installation in a new vehicle. This facilitates the whole process, because it should be borne in mind that the vehicle consists of different materials, starting from precious metals, different fluids and they all require special procedures. The complete problem is more complex due to the fact that manufacturers place new models on the market with some additional new materials. This especially applies to electric vehicles, gas vehicles, etc.

Annually in the EU, the disposal of vehicles at the end of the service life creates between 8 and 9 million tons of waste that must be properly managed. From that aspect, the Directive 2000/53/EC of the European Parliament and the European Council of the EU regulates the measures and logistics of dealing with ELV in order to protect the human environment and save the engaged energy. The Directive also restricts the re-use of certain parts that have been dismantled from decommissioned vehicles [8].

The Directive regulates the procedure for handing over a vehicle that has no market value (or is negative) by the last owner, to authorized recycling facilities, for which an appropriate Certificate is issued. At the same time, an appropriate financial incentive is prescribed by the vehicle manufacturer.

According to the requirements of the Directive (2000/53 / EC), the vehicle as a whole must contain a certain percentage of reusable parts and fluids and recyclable materials [8, 9].

2. BASIC CONSIDERATIONS ON THE PROCESS OF RECYCLING MOTOR VEHICLE

During the dismantling process (consisting of the collection, removal of unauthorized impurities and crushing) of ELVs in Europe, two main aspects must be taken into account:

- First, there is evidence to suggest that ELVs are being treated illegally in some cases; and

• Second, even in authorized recycling facilities, the classification of specific waste is not done properly and is not fully in line with the relevant requirements of the existing ELV Directive. Certain types of fluid in vehicle systems, such as brake fluids, windshield washer fluid, oil filters or shock absorbers, are not always disposed of in an environmentally friendly manner.

Also, it is necessary to properly separate the parts from hazardous substances such as mercury (Hg), which can be an integral part of the light group or switch, etc., and prevent their spillage into the environment.

Lead-acid batteries and acid are also dismantled from vehicles in a special way and treated in a special way because, in addition to their toxic properties, they can also damage shredders at recycling plants. The same applies to fuel tanks and airbags due to the presence of toxic and flammable gases.

Shredders are used for tearing to pieces and/or for shredding and crushing vehicles and parts. In general, after crushing, metal residues remain without the presence of hazardous substances. However, in practice, it has been shown the opposite and that impurities often appear.

An international standard (ISO 22628: 2002) defines a procedure for calculating the percentage of recyclability and reuse of installed materials within a new vehicle, calculated per unit mass of the vehicle [10].

The percentage of recyclability (R_{cyc}), or (recyclability indicator) of a motor vehicle, represents the percentage of mass (percentage by mass share), and can be calculated using the following equation (1):

$$R_{cyc} = \frac{m_P + m_D + m_M + m_{Tr}}{m_V} \cdot 100 \geq 85\% \qquad (1)$$

Percentage or indicator of reuse of embedded materials (R_{cov}), is calculated using the following equation (2):

$$R_{cov} = \frac{m_P + m_D + m_M + m_{Tr} + m_{Te}}{m_V} \cdot 100 \geq 95\% \qquad (2)$$

where:

- m_p - Mass of materials released during the vehicle recycling preparation process; (all liquids, batteries, oil filter, tires, catalysts, etc.);
- m_D - Mass of materials released during the vehicle disassembly process (large, easily replaceable parts made of polymeric materials and elastomers, such as bumpers, instrument panels, etc.);
- m_M - Mass of materials released during the process of crushing and separating metals;
- m_{Tr} - Mass of non-metallic materials, which are separated during the crushing process; and
- m_{Te} - Mass of non-metallic materials (polymeric materials and elastomers which are difficult to disassemble and which are lighter than 100-200 g, respectively), as well as other flammable materials (Leather, wood, card reader, etc.).

The time of disassembling the vehicle depends on the construction, the way of connecting individual parts of the construction, the technical instructions for disassembling, etc.

3. DEVELOPMENT OF RECYCLING CENTERS FOR MOTOR VEHICLE RECYCLING ON THE DOMESTIC MARKET

3. 1 Market projection of purchase of vehicles for recycling and sale of recycled materials

The market for the purchase of waste vehicles and for the sale of recycled materials primarily represents the territory of Serbia, and on the foreign market these are the former Republics of SFRY. It should be borne in mind that due to the announced abolition of imports and withdrawal from the use of obsolete vehicles. Therefore, an additional increase in the volume of activities in the field of recycling is forecast, that is planned dismantling and dismantling of obsolete vehicles.

Also, it should be taken into account the fact that the number of manufacturers of electric vehicles, as well as hybrid vehicles, is increasing.

At the same time, the turnover is increasing, that is the demand for recycled materials and the so-called repaired spare parts, in which, in our region, Slovenia leads, following the example of European and world countries.

3.2 Organization and optimization of the electric vehicles recycling process

Having in mind the increase in the number of electric vehicles, it is necessary to think about their recycling in a timely manner. Since electric vehicles contain additional parts and equipment that are not available on classic vehicles (electromagnets, batteries, etc.), it is necessary to invest part of the profit in the formation of a new separate plant for dismantling and recycling electric vehicles. In that way, the company would remain competitive on the market. The concept of one such plant is shown in Figure 2 [11].

The goal is to further adapt the existing plant within the company for recycling motor vehicles with classic engines by networking the part for disassembly of electric vehicles. Within the additional network, the issue of recycling electric batteries has been developed a lot [11]. Emphasis is placed here on disassembling electric motors, separating magnets, their depolarization and reuse.

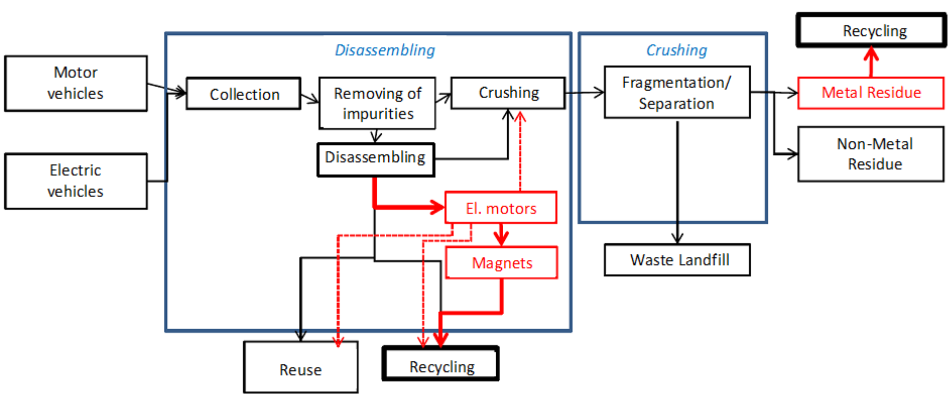

Figure 2: *Pilot plant for recycling electric vehicles with preparation for separation and reuse of permanent magnets*

The complete plant consists of a receiving department, a sector for disassembling vehicles and part for disassembling electric vehicles and separating electric motors and magnets. After crushing, metal and non-metal parts are separated and materials that cannot be used further are deposited.

Considering that it is the obligation of the designer to select recyclable materials on the designer's table, it can be expected that the share of plastics and plastic materials will have a declining trend in the coming years.

As there is a growing problem today in the recycling of plastic materials, especially polyvinyl chloride (PVC), a number of manufacturers are replacing this type of material with various alloys, especially aluminum alloys. The use of aluminum in motor vehicles (especially passenger vehicles) has been constantly increasing in recent years. Thus, in 1998, the average amount of aluminum was 85 kg per vehicle, while in 2008 it was about 160 kg per vehicle [12-14]. For now, the greatest application of aluminum is in the manufacture of engines, transmissions and bodies, especially in vehicles of higher class.

Aluminum has been proven to be completely recyclable, with the recycled material fully retaining all its characteristics, which is another advantage of this metal. Due to these favorable characteristics, aluminum is increasingly used in the automotive industry. In the USA, for example, the trend of increasing the use of aluminum lasts over 50 years and it is predicted that by 2028, about 256 kg of this metal will be installed in passenger and light trucks, Figure 3 [15-17]

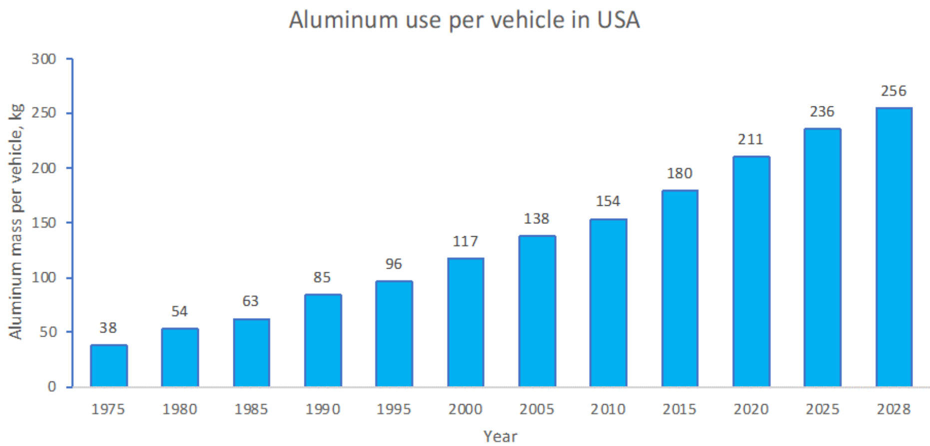

Figure 3: *Trend of Al use in passenger and light truck vehicles in the USA*

Also, it is predicted that by 2030, about 10 million tons of aluminum will be installed in electric and hybrid vehicles, which is 10 times more than the current situation. As an example, the e-Golf is equipped with about 129 kg of aluminum, the Nissan Leaf 171 kg, while the luxury model Tesla S has about 661 kg of this metal [15-17].

3.3 Motor vehicle recycling process after use

It is important to note that regardless of whether the recycling process is performed with prior disassembling of the vehicle, or the vehicles are delivered directly for crushing, the removal of hazardous materials and materials from vehicles that may endanger the environment must be performed before any procedure (Depollution process). This is defined in Annex 1 of Directive 2000/53/EC, Article 6. Directive 2000/53/EC stipulates that all materials and fluids that can pollute the environment must first be removed from waste vehicles and only then can they be sent to waste or crushing. Annex 1 of Directive 2000/53/EC specifies what such a procedure must include [8]:

- Removal of batteries, tanks for conventional fuels (petrol and diesel) or tanks for alternative fuels (liquefied petroleum gas, hydrogen, methane);
- Removal and neutralization of potentially explosive components (for example airbags, gas shock absorbers);
- Removal, separation, collection and storage of fuels, motor oils, gear oils, differential oils, hydraulic oils, coolants, brake oils, fluids from the vehicle air conditioning system, as well as all other fluids and fluids that may be found in waste vehicle; and
- Removal of components containing mercury and other toxic materials.

After this procedure, waste vehicles are transported to special plants that are intended for grinding and crushing, the so-called shredders. The vehicle is transported and compacted in a shredder where it is broken and torn into pieces the size of a few centimeters, which enables easier recycling of materials that are part of the vehicle and recovery of up to approximately 80% of the material. After grinding and crushing the vehicle, the materials are separated and divided, usually into metals and non-metals [18].

The maximum thickness of materials processed in the Shredder plant is 2 mm for sheet metal, 5 mm for steel and 10 mm for circular parts. In Figure 4, a schematic representation of the Shredder metal waste recycling plant is given [18, 19].

Prior to processing in the Shredder, the materials must be free of explosive, flammable, toxic and chemically aggressive liquids, gases and dust.

Before crushing the vehicle in the Shredder plant, the following are removed: windows, battery, electronics and electrical installation, tires, plastic parts (bumpers), fuel tank, air conditioning, waste oils in the gearbox, shock absorbers, brake system, engine, power steering device, etc.

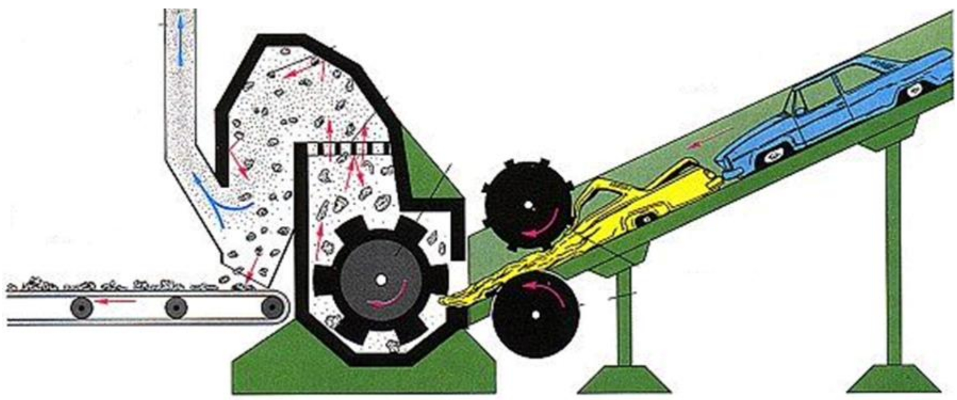

Figure 4: *Shredder Plant for recycling vehicles and scrap metal*

The basic products of recycling old passenger cars in the Shredder plant are, Figure 5 [18-20]:

- Magnetic waste fractions (iron and steel) about 70%;
- Mixed fractions of non-magnetic metals (aluminum, copper, etc.) maximum 6.4%;

- Light fractions from Shredder plants (PVC, elastomers, polyurethane, glass, ceramics, paints, etc.) about 23%; and
- Iron with copper content of 0.2% to 0.3% that can be used for production of less useful steel (about 0.6%).

Figure 5: *Products of recycling old vehicles in Shredder plant*

4. CONCLUSIONS

The transport sector is responsible for one quarter of the total greenhouse gas emissions in the European Union. The largest emission is generated by the energy sector, followed by transport, industry, households, agriculture and others.

The Directive of the European Parliament and of the Council Directive 2000/53/EC regulates waste management in the vehicle sector. Appropriate regulations thus regulate the procedures from writing off the vehicle to disassembling the vehicle into its component parts, their classification, recycling and re-installation in a new vehicle.

The International Standard (ISO 22628:2002) defines a procedure for calculating the percentage of recyclability and reuse of installed materials within a new vehicle, calculated per unit of mass of the vehicle. The method is harmonized by the motor vehicle manufacturers and is applicable to each new manufactured vehicle.

Through its activities, the new recycling center for recycling electric vehicles should contribute to the development of the domestic material market through ecological disassembling and dismantling of obsolete vehicles, which parts are further recycled and reused. Since electric vehicles contain additional parts and equipment that are not available on classic vehicles (electromagnets, batteries, etc.), it is necessary to invest part of the profit in the formation of a new separate plant for disassembling and recycling electric vehicles.

As today there is a growing problem in the recycling of plastic materials, especially polyvinyl chloride (PVC), a number of manufacturers are replacing this type of material with various alloys, especially aluminum alloys. The use of aluminum in motor vehicles (especially passenger vehicles) has been constantly increasing in recent years. Aluminum has been proven to be completely recyclable, with the recycled material fully retaining all its characteristics, which is another advantage of this metal.

ACKNOWLEDGMENT

This paper is a result of the researches within the project TR35041 financed by the Ministry of Science and Technological development of the Republic of Serbia.

REFERENCES

[1] European Commission: Reducing emissions from transport. A European Strategy for low- emission mobility, http://ec.europa.eu/clima/policies/transport_en, accessed on: august 2020

[2] Jette Krause, Christian Thiel, Dimitrios Tsokolis, Zissis Samaras, Christian Rota, Andy Ward, Peter Prenninger, Thierry Coosemans, Stephan Neugebauer, Wim Verhoeve, EU road vehicle energy consumption and CO2 emissions by 2050 – Expert-based scenarios, Energy Policy, Volume 138, 2020, 111224, ISSN 0301-4215, https://doi.org/10.1016/j.enpol.2019.111224

[3] Skrúcaný T, Kendra M, Stopka O, Milojević S, Figlus T, Csiszár C (2019) Impact of the Electric Mobility Implementation on the Greenhouse Gases Production in Central European Countries. Sustainability 11:4948. https://doi.org/10.3390/su11184948

[4] Milojević S and Pešić R 2011 CNG buses for clean and economical city transport, *Int. J. Mobility and Vehicle Mechanics (MVM)* **37**(4) 57-71, http://www.mvm.fink.rs/Journal/Archive/2011/2011V37N4/4_sasa_milojevic/milojevic_pesic_rad.pdf

[5] Milojević S 2016 Reconstruction of existing city buses on diesel fuel for drive on Hydrogen, *Applied Engineering Letters* **1**(1) 16-23, https://www.aeletters.com/reconstruction-of-existing-city-buses-on-diesel-fuel-for-drive-on-hydrogen/

[6] Milojevic, S., Pesic, R. Theoretical and experimental analysis of a CNG cylinder rack connection to a bus roof. *Int.J Automot. Technol.* **13,** 497–503 (2012). https://doi.org/10.1007/s12239-012-0047-y

[7] Xue, Y.; Guan, H.; Corey, J.; Zhang, B.; Yan, H.; Han, Y.; Qin, H. Transport Emissions and Energy Consumption Impacts of Private Capital Investment in Public Transport. *Sustainability* 2017, *9*, 1760. https://doi.org/10.3390/su9101760

[8] Directive 2000/53/EC of the European Parliament and of the Council of 18 September 2000 on end-of life vehicles, 2008, Council of the European Union and European Parliament, https://eur-lex.europa.eu/legal-content/EN/TXT/HTML/?uri=CELEX:32000L0053&from=EN

[9] Bukvić M, Stojanović B, Ivanović L and Milojević S 2017 Recycling of the Hybrid and Electric Vehicles, *Acta Technica Corviniensis - Bulletin Of Engineering* **10**(3) 107-114, http://acta.fih.upt.ro/pdf/2017-3/ACTA-2017-3-16.pdf

[10] ISO 22628:2002(en), Road vehicles — Recyclability and recoverability — Calculation method, https://www.iso.org/obp/ui/#iso:std:iso:22628:ed-1:v1:en

[11] Milojević I (2020) Optimization of Communication Flows of Electric Vehicle Recycling Processes and their Specific Equipment. Master thesis, University of Kragujevac, Faculty of Engineering

[12] Mohan, T.V.K., Amit, R.K. Dismantlers' dilemma in end-of-life vehicle recycling markets: a system dynamics model. *Ann Oper Res* **290,** 591–619 (2020) https://doi.org/10.1007/s10479-018-2930-z

[13] Li, Y.; Fujikawa, K.; Wang, J.; Li, X.; Ju, Y.; Chen, C. The Potential and Trend of End-Of-Life Passenger Vehicles Recycling in China. *Sustainability* **2020**, *12*, 1455, https://doi.org/10.3390/su12041455

[14] S Milojevic *et al* 2019 Vehicles optimization regarding to requirements of recycling *Example: Bus dashboard, IOP Conf. Ser.: Mater. Sci. Eng.* **659** 012051, https://doi.org/10.1088/1757-899X/659/1/012051

[15] Sandra Veličković, Blaža Stojanović, Lozica Ivanović, Slavica Miladinović, Saša Milojević 2019 Application of nanocomposites in the automotive industry, Int. J. Mobility and Vehicle Mechanics (MVM) 45(3) 51-64, https://doi.org/10.24874/mvm.2019.45.03.05

[16] B. Stojanovic, M. Bukvic, I. Epler 2018 Application of aluminum and aluminum alloys in engineering, *Applied Engineering Letters* **3**(2) 52-62, https://www.aeletters.com/wp-content/uploads/2018/10/AEL00069.pdf

[17] Zeng, X., Li, M., Abd El-Hady, D., Alshitari, W., Al-Bogami, A. S., Lu, J., Amine, K., Commercialization of Lithium Battery Technologies for Electric Vehicles. *Adv. Energy Mater.* 2019, 9, 1900161. https://doi.org/10.1002/aenm.201900161

[18] Everett J.W. (2012) Waste Collection and Transport. In: Meyers R.A. (eds) Encyclopedia of Sustainability Science and Technology. Springer, New York, NY. https://doi.org/10.1007/978-1-4419-0851-3_124

[19] Vladimir Simic, Branka Dimitrijevic. Production planning for vehicle recycling factories in the EU legislative and global business environments. *Resources, Conservation and Recycling* 2012, *60*, pp. 78-88. https://doi.org/10.1016/j.resconrec.2011.11.012

[20] Sakai, S., Yoshida, H., Hiratsuka, J. *et al.* An international comparative study of end-of-life vehicle (ELV) recycling systems. *J Mater Cycles Waste Manag* **16,** 1–20 (2014). https://doi.org/10.1007/s10163-013-0173-2

MOBILITY & VEHICLE MECHANICS

DOI:10.24874/mvm.2020.46.02.04
UDC: 629.3.015.5

CONTRIBUTION TO RESEARCH OF SPECIFIC PRESSURE BETWEEN TIRE AND ROAD IN MOTOR VEHICLES

Miroslav Demić[1], Danijela Miloradović[2]

Received in July 2020 Accepted in September 2020

RESEARCH ARTICLE

ABSTRACT: One of the most important features of special motor vehicles is the possibility of movement outside the regular roads. In order to provide appropriate characteristics of mobility, such vehicles should, among other things, meet the requirements in terms of geometric parameters of mobility, traction characteristics, characteristics of stability, and the possibility of overcoming obstacles. As the contact between the tire and the road is very important for ensuring proper performance of motor vehicles, significant attention must be paid to it. Keeping this in mind, a model for approximation of average specific pressure between the tire and the deformable surface has been identified in this paper. In the coming period, research that is more detailed should be carried out in order to define similar models for different tires and road surfaces.

KEY WORDS: vehicle, tire, air pressure, radial load, average specific pressure

[1] *Miroslav Demić, PhD., prof., Academy of engineering sciences of Serbia, Kraljice Marije 16, 11000 Belgrade, Serbia, e-mail: demic@kg.ac.rs*
[2] *Danijela Miloradović, PhD., assoc. prof., University of Kragujevac, Faculty of engineering, Sestre Janjić 6, 34000 Kragujevac, e-mail: neja@kg.ac.rs, (*corresponding author)*

PRILOG ISTRAŽIVANJU SPECIFIČNOG PRITISKA IZMEĐU PNEUMATIKA I TLA KOD MOTORNIH VOZILA

REZIME: Jedna od najvažnijih karakteristika specijalnih motornih vozila je mogućnost kretanja van uređenih saobraćajnica. Da bi se obezbedile odgovarajuće karakteristike prohodnosti, takva vozila treba da, između ostalog, ispune zahteve u pogledu geometrijskih parametara prohodnosti, vučnih karakteristika, karakteristika stabilnosti, kao i mogućnosti savladavanja prepreka. Kako je kontakt pneumatika i tla veoma značajan za obezbeđivanje odgovarajućih performansi motornih vozila, njemu se mora posvetiti značajna pažnja. Imajući to u vidu, u ovom radu je identifikovan model za aproksimaciju srednjeg specifičnog pritiska između pneumatika i deformabilne podloge. U narednom periodu treba izvršiti detaljnija istraživanja sa ciljem da se slični modeli definišu za različite pneumatike i podloge-puteve.

KLJUČNE REČI: vozilo, pneumatik, pritisak vazduha, radijalno opterećenje, srednji specifični pritisak

CONTRIBUTION TO RESEARCH OF SPECIFIC PRESSURE BETWEEN TIRE AND ROAD IN MOTOR VEHICLES

Miroslav Demić, Danijela Miloradović

1. INTRODUCTION

One of the most important features of special motor vehicles is the possibility of movement outside the regular roads. In order to provide appropriate characteristics of mobility, such vehicles should, among other things, meet the requirements in terms of geometric parameters of mobility, traction characteristics, characteristics of stability, and the possibility of overcoming obstacles. These wheeled vehicles are often equipped with special tires and systems for central air pressure regulation [1]. These systems, in addition to providing smaller specific pressure, also provide greater reliability of tires, as they provide compensation for air loss that can be caused by punctured tires.

The design of the tires should ensure, among other things, the lowest possible specific pressure. As the contact between the tire and the road is very important for ensuring the appropriate performance of motor vehicles, considerable attention must be paid to it [2-8]. Since the aim of this paper is to develop a method for calculating the specific pressure between the tire and the road, the results of some previous research will be considered.

The problem of contact between the tires and the dirt roads is explained in detail in [3]. The results of experimental research on truck tires have shown that as the tire air pressure and the radial load increase, the average specific pressure between the tire and the road also increases.

The book [9] is completely dedicated to terramechanics, especially to the calculation and measurement of actual road loads in various types of vehicles (military vehicles, trucks, passenger vehicles, tractors, etc.). The relationship between the tires and the deformable surface is especially emphasized.

In [10], the authors point out the importance of research of the relationship between the tire and deformable ground in trucks. A method for measurement of tire footprints on deformable ground and a software for data analysis have been developed.

The authors of [11] give an overview of conventional and unconventional procedures for measuring the specific pressure between the tires and the road. A method based on acoustic phenomena is specifically described.

The problem of modelling the relationship between the tires and the road was specifically considered in [12], while the interaction between the tires and the ground from the aspect of the influence of different types of road surface on the characteristics of motor vehicles was discussed in detail in [13].

In [14], the author investigates in detail the influence of the contact and the ground on the performance of agricultural tractors.

Considering the reviews of some of the materials published in this field, the conclusion can be made that this problem is still relevant today, especially with freight motor vehicles intended for off-road driving, as well as with agricultural machinery. Therefore, an acceptable model of average specific pressure between the tires and the deformable ground was defined in the paper, based on the existing experimental results from [3].

2. APPLIED METHOD

For further analysis, data from [3] are shown in Figure 1. They refer to the contact of the truck tire 11.00 R16XL and deformable ground (dirt road) with precisely defined composition of clay and sand, at different tire air pressures and different radial loads.

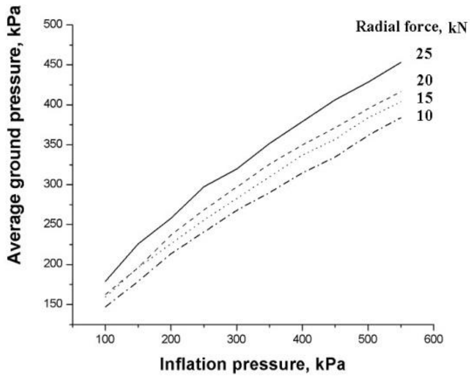

Figure 1: *Dependence of average specific pressure on tire radial force and tire inflation pressure* [3]

The analysis of data from Figure 1 shows that the average specific pressure between the tire and the ground increases with the increase of the tire inflation pressure and this is also happening with the increase in radial force.

Data from Figure 1 were digitized using the PlotDigitizer software and displayed in the form of 3D graphics in Figure 2.

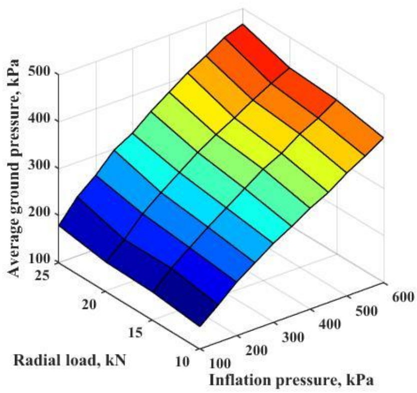

Figure 2: *3D graphics of dependence of the average specific pressure between the tire and the road on tire inflation pressure and radial force of data from [3]*

Figures 1 and 2 show that the dependence of the average specific pressure on tire inflation pressure and radial force is defined at a relatively small number of points, which is not sufficient for more precise analyses. In order to improve the accuracy, the number of points where the surface is defined is increased, so data from Figure 2 were approximated by 2D spline transforms and shown in 256x256 points, Figure 3.

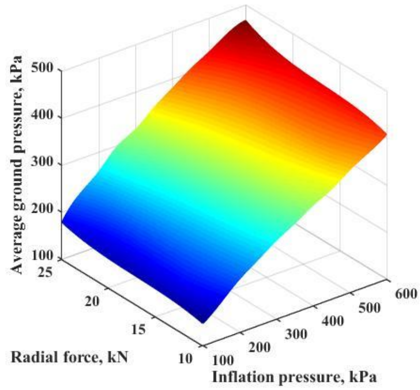

Figure 3: *Approximated data on dependence of average specific pressure between the tire and the road on tire inflation pressure and radial force defined in 256x256 points*

As average specific pressure from Figures 2 and 3 depends on two quantities - tire inflation pressure and radial force, their frequency spectra were also included in the analysis. Therefore, a 2D Fourier transform was performed using OriginPro software. The mentioned transform was performed for the data shown in Figure 3. Since information about the process is mainly carried out by the magnitude of the 2D Fourier transformation spectrum [15], the magnitude is shown, for illustration, in Figure 4.

Analysis of the data from Figure 4 shows the way the magnitude of the spectrum changes with the change of tire inflation pressure and radial force frequency. The peaks appear at the coordinate origin (p_{min}, Z_{min}) and at the points (p_{max}, Z_{max}) and (p_{min}, Z_{max}), where:

- p_{min}, p_{max}, kPa^{-1} are minimum and maximum inflation pressure frequency and
- Z_{min}, Z_{max}, kN^{-1} are minimum and maximum radial force frequency.

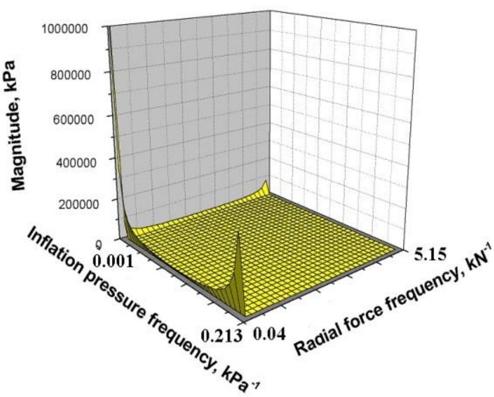

Figure 4: *Spectrum magnitude of 2D Fourier transform of approximated data*

Considering the previous analysis, further research was oriented on modelling the experimental data from Figure 1, using the “black box” method. The experimental data are represented by a function with unknown parameters, which are calculated using one of the identification methods [16-19].

To define the structure of the model, research was conducted with different polynomial shapes, and preliminary analyses showed that the smallest error occurs with the following model:

$$p_{spc} = \left(x_1 + x_2 \cdot p + x_3 \cdot p^2 + x_4 \cdot p^3\right) \cdot \left(x_5 + x_6 \cdot Z + x_7 \cdot Z^2 + x_8 \cdot Z^3\right), \tag{1}$$

where:

- p_{spc} is specific pressure, kPa,
- p is tire inflation pressure, kPa,
- Z is radial tire force, kN,
- x_i, $i = 1,8$ are polynomial parameters that should be identified.

The identification of unknown model parameters of the average specific pressure between the tire and the ground was performed using the identification method based on optimization principles [16], the block diagram of which is shown in Figure 5.

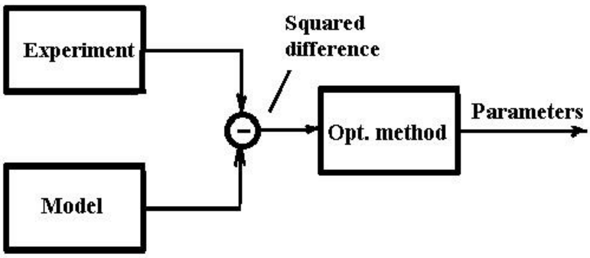

Figure 5: *Block diagram of the used method for identification of the parameters of the model for average specific pressure between the tire and the road*

Figure 5 shows that, in order to identify the parameters of the model of the mean specific pressure between the tire and the ground, it is necessary to have the results of experimental research. In this case, experimental data from [3] were used. Measurement errors were not taken into account, so they are not shown in the figure.

In order to identify the parameters of the model (1), the objective function was defined in the form of the square of the differences (2), and the unknown parameters were determined from the conditions of its minimization.

$$\Phi = \Sigma\left[p_{spc} - p_{\exp}\right]^2. \tag{2}$$

Minimization of the objective function was performed by the optimization method, whose block diagram is shown in Figure 6. The method itself is described in detail in [10-13].

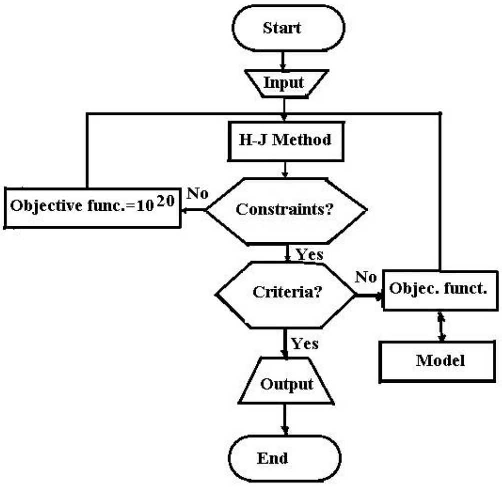

Figure 6: *Block diagram of the optimization method*

In this particular case, the Hooke-Jeeves method was used for optimization. During the process of parameter identification, penal functions [18] were used, with the introduction of limits of the parameter values $x_i \in [-100, 200]$, with the search step for the objective function of 10^{-5} and with the criterion of interrupting the iteration process of the Hooke-Jeeves method of 10^{-10}.

3. DATA ANALYSIS

Model parameters were calculated from the expressions (1) and (2) and listed in Table 1.

Table 1: *Identified parameters of the model (1)*

	X_1, kPa	X_2, –	X_3, kPa^{-1}	X_4, kPa^{-2}	X_5, –	X_6, kN^{-1}	X_7, kN^{-2}	X_8, kN^{-3}
	$2,05 \cdot 10^{3}$	$2,95$	$-6,77 \cdot 10^{-3}$	$6,7 \cdot 10^{-6}$	$-1,84 \cdot 10^{-2}$	$1,16 \cdot 10^{-2}$	$-2,53 \cdot 10^{-4}$	$3,14 \cdot 10^{-6}$

Minimum value of the objective function of $2,908 \cdot 10^{2}$ was calculated after 59 922 402 iterations.

Values of the mean specific pressure calculated at 256x256 points for the identified model parameters from Table 1 and based on expression (1), are shown in Figure 7. Analysis of data from Figures 3 and 7 shows that they preliminary describe data from Figure 3 with acceptable accuracy.

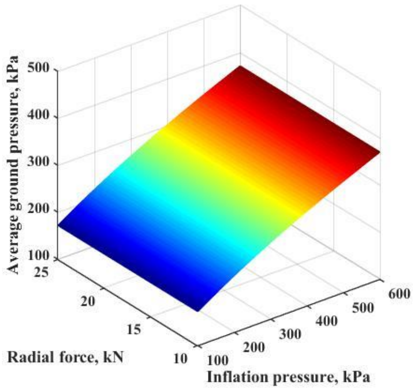

Figure 7: *3D chart of the model defined in 256x256 points*

In order to support this claim, relative errors of the model in relation to the initial experimental data [3] were calculated and presented in Figure 8.

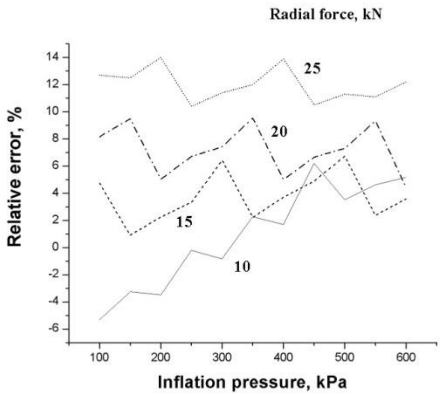

Figure 8: *Relative error of the model in relation to initial data from [3]*

By analysing data from Figure 8, it can be determined that the relative error ranges from -6% to 14% for the observed values of tire inflation pressure and radial force. The interval of relative errors is acceptable for identification of mathematical models.

For further analyses, a 2D Fourier transform was performed of the data shown in Figure 7, and the obtained spectrum magnitudes are shown in Figure 9.

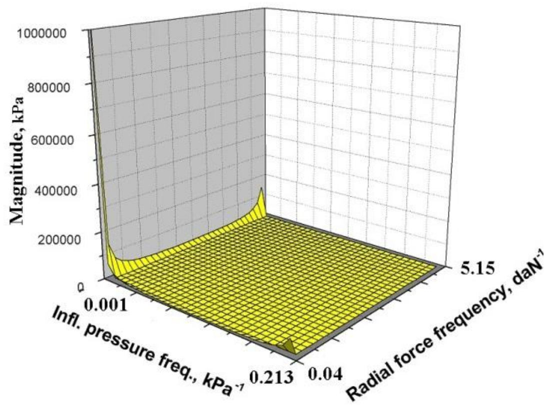

Figure 9: *Magnitude of 2D Fourier transform spectrum obtained using the model (1) in 256x256 points*

The analysis shows that there is a great similarity in character of data from Figures 4 and 9. This indicates that model (1) approximates data from Figure 3 in the frequency domain in satisfactory manner. Thus, it can be stated that the identified model can be used in the case of vehicles with tires of approximately the same dimensions when driving on a deformable surface. In the following period, a more detailed research should be performed in order to define similar models for different tires and road surfaces.

Finally, it should be noted that the procedure for calculating statistical errors is defined for the 1D Fourier transform in [20], while such procedures for Fourier transforms with multiple variables do not exist, so the analysis of the mentioned errors was not performed in this paper.

4. CONCLUSIONS

Based on the performed research, it can be concluded that the developed model of mean specific pressure between tires and deformable surface enables dynamic simulation with acceptable relative error. The identified model can be used in the case of vehicles with tires of approximately the same dimensions, when moving on a deformable surface. In the following period, a more detailed research should be performed in order to define similar models for different tires and road surfaces.

ACKNOWLEDGMENT

This paper is a result of the researches within the project TR35041 financed by the Ministry of Science and Technological development of the Republic of Serbia.

REFERENCES

[1] FAP. Information: Technical data (in Serbian). Priboj: FAP, 1972-2013.

[2] Demić, M. and Lukić, J. Theory of motor vehicle motion (in Serbian). Kragujevac: Faculty of mechanical engineering, 2011. ISBN 978-86-86663-54-2.

[3] Wong, J. Y. Theory of ground vehicles, 4th ed., New York: John Wiley & Sons Inc., 2001. ISBN 0-471-35461-9.

[4] Mitschke, M. and Wallentowitz, H. Dynamik der Kraftfahrzeuge. Wiesbaden: Springer Verlag, 2014. ISBN 978-3-658-05067-2.

[5] Genta, A.: Motor Vehicle Dynamics. Singapore: World Scientific Publishing Co. Pte.. Ltd., 2003. ISBN 9810229119.

[6] Gillespie, TD. Fundamentals of Vehicle Dynamics. Warrendale: SAE, 1992. ISBN 978-1-56091-199-9.

[7] Miliken, WF. and Miliken, DL.: Race Car Vehicle Dynamics. Warrendale: SAE, 1995. ISBN 1-56091-526-9.

[8] Simić, D. Motor vehicle dynamics (in Serbian), Belgrade: Naučna knjiga, 1988. ISBN 86-23-43026-3.

[9] Pytka, JA. Dynamics of wheel–soil systems: A soil stress and deformation-based approach. Boca Raton: CRC Press, 2013. eBook ISBN 9780429087103.

[10] Arshad, AK. et al. Pavement response to variable tyre pressure of heavy vehicles. In: Rahman NA. et al. (Eds.). Proceedings of the 3rd international conference on civil and environmental engineering for sustainability (IConCEES 2015). Paris: EDP Sciences, 2016, 47, Paper No. 03009. DOI: https://doi.org/10.1051/matecconf/20164703009 .

[11] Wang, Q. et al. (2012). Dynamic Tire Pressure Sensor for Measuring Ground Vibration, Sensors. Basel: MDPI, 2012, 12(11), 15192-15205; DOI: 10.3390/s121115192.

[12] Cui, K. et al. A new approach for modelling vertical stress distribution at the soil/tyre interface to predict the compaction of cultivated soils by using the PLAXIS code, Soil and Tillage Research. Amsterdam: Elsevier B.V., 2006, 95(1-2), 277–287. DOI: https://doi.org/10.1016/j.still.2007.01.010

[13] Nemchinov, M.V. et al. Road wheel interaction (in Russian), Наука и техника в дорожной отрасли. Moscow: ЗАО Издательство Дороги, 2014, 2, 12-14.

[14] Muzikravić, V. (2005). Exploring the possibility of adapting agricultural tractors to the conditions of exploitation from the aspect of traction optimization (in Serbian). Novi Sad: Faculty of technical sciences, 2005. Ph.D. thesis, University of Novi Sad.

[15] Acharya, T. et al. (2005) Image Processing - Principles and Applications, New York: John Wiley & Sons, 2005. ISBN 978-0-471-71998-4

[16] Bunday, BD. Basic optimization methods. Hoboken: Hodder Arnold, 1984. ISBN 978-0713135060.

[17] Demić, M. Optimisation of motor vehicles vibration parameters (in Serbian). Kragujevac: Faculty of mechanical engineering, 1997. ISBN 86-81745-40-9.

[18] Demić, M.: Optimization of Vehicles Elasto-Damping Element Characteristics from the Aspect of Ride Comfort. Vehicle System Dynamics, 1994, 23(1), 351-377. DOI: 10.1080/00423119408969066.

[19] Demić, M. Identification of Vibration Parameters for Motor Vehicles. Vehicle System Dynamics, 1997, 27(2), 65-88. https://doi.org/10.1080/00423119708969323

[20] Bendat, JS. and Piersol, AG. Random Data - Analysis and measurement procedures. London: John Wiley and Sons, 2000. ISBN: 978-0-470-24877-5.

MOBILITY & VEHICLE MECHANICS

DOI:10.24874/mvm.2020.46.02.05
UDC: 629.3.027.2

STEERING SYSTEM DESIGN OF THE SECOND GENERATION FORMULA SAE

Mobin Majeed[1], *Greg Wheatley*[2]

Received in July 2020 Accepted in August 2020

RESEARCH ARTICLE

ABSTRACT: The aim of this paper is to design the steering system of the formula racing car. This includes the designing of its main components in SolidWorks, its analysis by calculation and finite element simulation. Load acting on the wheels of formula car are calculated and input in the analysis wherever necessary. The cars steering rack is repositioned to avoid any collision with a-arms. The force acting on the bolts at tie rod, clevis and mounting bracket is found below its yield strength. The clevis attached at the end of the rack is subject to load and fatigue analysis in ANSYS and all results were found satisfactory. Similar analysis is done for rack arm at critical areas and its was found that region where the rack arm can withstand fluctuations ranging for almost whole life till failure.

Later the whole steering system was split into three major components (Steering column assembly, steering rack assembly, Tie rod assemblies) and each component is designed separately in SolidWorks and then assembled into whole one. SKF SAKAC 10 M ends are selected rod ends for steering arm assembly allowing rigid force transfer between rack arms and upright assembly as well as vertical motion of wheel assembly in operation. In the assembly 6 x M8 and 4 x M10 exist with the associated washers and nuts. The universal joint connecting the two steering column was machined according to Australian standards with splines at both ends. Two splined steering columns was machined in order to complete the steering column assembly. In order to stop the clevis colliding with the steering with the rack on full lock and to restrict the steering of the vehicle two locking collars were manufactured.

KEY WORDS: Steering assembly, rack and pinion, design, fatigue, ANSYS, SOLIDWORKS

[1] *Mobin Majeed, Ph.D. student, James Cook University mobeen414@gmail.com*
[2] *Greg Wheatley, PhD, Senior Lecturer, James Cook University, greg.wheatley@jcu.edu.au, (*corresponding author)*

DIZAJN UPRAVLJAČKOG SISTEMA DRUGE GENERACIJE FORMULE SAE

REZIME: Cilj ovog rada je da osmisli sistem upravljanja vozila formule. To uključuje projektovanje njegovih glavnih komponenata u paketu SolidWorks, njegovu numeričku analizu i simulaciju metodom konačnih elemenata. Opterećenje koje deluje na točkove vozila formule se proračunava i unosi u analizu kad god je to potrebno. Letva upravljača vozila postavljena je tako da izbegne bilo kakav kontakt sa A vođicom. Sila koja deluje na zavrtanj na sponi, čauri i nosaču nalazi je niža od granice tečenja. Spona pričvršćena na kraj letve podvrgnuta je analizi opterećenja i zamora u ANSYS-u. Utvrđeno je da su svi rezultati zadovoljavaju postavljene kriterijume. Slična analiza je rađena za sponu u kritičnim presecima i rezultati su pokazali da u toj oblasti spona može podneti fluktuacije opterećenja tokom celog životnog ciklusa do otkaza.

Kasnije je ceo sistem upravljanja podeljen na tri glavne komponente (sklop stuba upravljača, sklop letve upravljača, sklopovi spona). Svaka komponenta je dizajnirana odvojeno u SolidWorks, a zatim su sastavljene u celinu. Zglobna SKF SAKAC 10 M je izabran za kraj upravljačke letve koji omogućuje kruti prenos sile između upravljačke letve i gornjeg sklopa, kao i vertikalno kretanje sklopa točkova u radu. U sklopu se nalazi još 6 x M8 i 4 x M10 sa pripadajućim navrtkama i podloškama. Zglob koji povezuje dva dela stuba upravljača je izrađen je prema australijskim standardima za navoje na oba kraja. Dva zaobljena dela stuba upravljača su dodatno obrađena. Kako bi se sprečilo zaključavanje dodata su dva elementa da spreče zaključavanje.

KLJUČNE REČI: Upravljački sklop, letva i zupčanik, dizajn, zamor, ANSYS, SOLIDWORKS

STEERING SYSTEM DESIGN OF THE SECOND GENERATION FORMULA SAE

Mobin Majeed, Greg Wheatle

INTRODUCTION

The purpose of this research paper is to design steering assembly of formula racing car. Aspects of the first generation car will be implemented into the second generation design with additional improvements to the vehicles maneuverability, handling and steering system safety. Steering system is being designed by carefully adhering to the rules of Formula SAE rule book and Australian standards. The steering system such as rack and pinion mechanism, steering wheel, steering column, tie rods as well as all necessary joints is fully designed in SOLIDWORKS and later analyzed in ANSYS. The major changes were to incorporate the current rack and pinion mechanism, move from its current position to avoid conflicts with driver's leg.

DESIGN APPROACH

The rules for the FSAE competition act as a constraint on the design of the steering system. According to the FSAE rule for Driver's leg and protection all moving components of the steering system including the steering rack and tie rods must be repositioned away from the driver's legs for driver safety[1]. All threaded fasteners utilized in the steering system must meet or exceed, SAE Grade 5, Metric Grade 8.8 and/or AN/MS specifications.

The Australian Standards that apply are listed in **Error! Reference source not found.** . Shaft sizes were determined using AS1402-2003. Standards 1665 and 1551 were referred to decide weld standards required to weld the mounting bracket with the frame of the car. Bolts used to mount the rack to the mounting bracket conform to product grades A and B in AS1110.1 (also listed in FSAE fastener regulations in the previous section). The mounting bracket and steering column of shaft were manufactured using 4140 choromoly with machinability specifications in accordance with AS1444-2007.

Table 1: Australian standard for design[2][3]

	Australian Standards
•	Australian Design Rule 10/02 — Steering Column
•	Australian Welding Code of Practice
•	AS1551-2011 - Welding of steel structures
•	AS1866 - Aluminium and Aluminium alloys
•	AS1665 - Welding of Aluminium structures
•	AS4024.1401 – Ergonomic Principles
•	AS1554.1 - Structural Steel Welding
•	AS1110.1 – Bolts
•	AS1444 – Wrought Allow Steels

The steering system was being designed parallel with other components of a car, so a discussion with other teams need to be had in order determine additional design constraints. Steering system tie rod connects directly to the upright to direct the front wheel, so the dimensions and solid works models of the upright geometry was needed to be obtained and analyze to understand the design constraints implemented by the upright team. Approximate dimensions for the JCUM driver was also needed to be attained in order to reposition the rack and pinion mechanism, steering column and tie rods without constricting the cockpit space of the driver[4][5].

DESIGN PROCESS

The design trend for the steering systems in competition remain relatively constant since long time[6]. All designs have a rack and pinion mechanism with complex packaging due to its high precision[3]. Most of the designed cited have their tie rod in line with the rack gear that reduces the bending stress[7]. A complete steering system design provided by our team leader is illustrated in the following **Figure 1**.

Figure 1: *a) Rack and pinion mechanism b) Formula car*

The second generation had mitigated the steering problems associated with the first generation formula car. The three major concepts are

- Minimizing overall effort of driver into the steering wheel[8]
- The driving space and steering system must be ergonomically feasible for the driver[9]
- Reduce stress on mounts and associated bushes
- Better Ackerman steering effect
- Smooth maneuverability

Three designs of steering wheel with rack and pinion connections are proposed. In the first design (**Figure 2**a) the universal joint is completely removed from the system for direct energy transfer. But the greater angled steering is ergonomically not feasible and cumbersome for driving. Second design (**Figure 2**b) consists of a single universal joint to improve high angled steering. The assembly is positioned to make two shaft lengths nearly equal for better distributing the forces. While the third design proposes two universal joint in the steering system (**Figure 2**c).

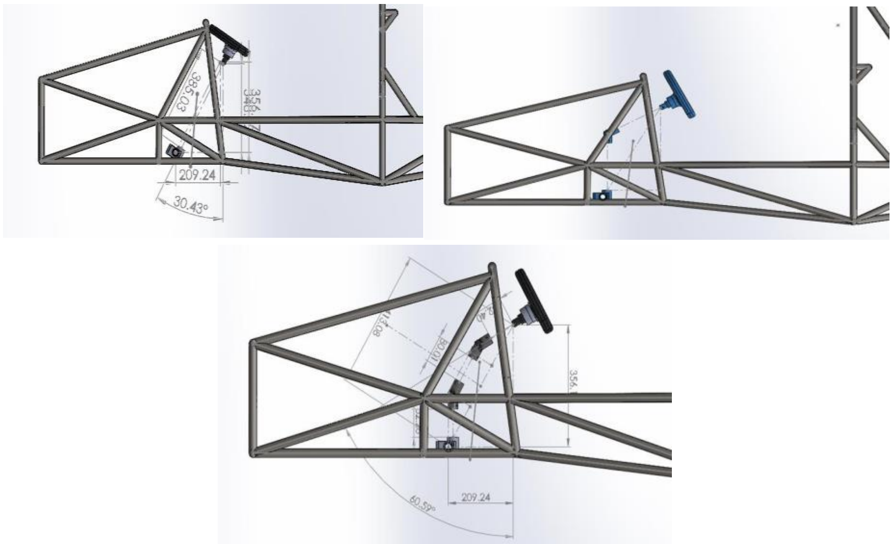

Figure 2:*a) System without universal joint b) with universal joint c) with two universal joint*

Furthermore, the preliminary design aims to position the steering rack such that the tie rods would run in line with the rack gear of the steering rack to the uprights[1]. But as the vehicle a-arms are also attached to the upright, this could result in collision especially in bumpy terrain[10]. So, the steering rack was repositioned further forward along the bottom strut of car frame as depicted in figure below (**Figure 3**).

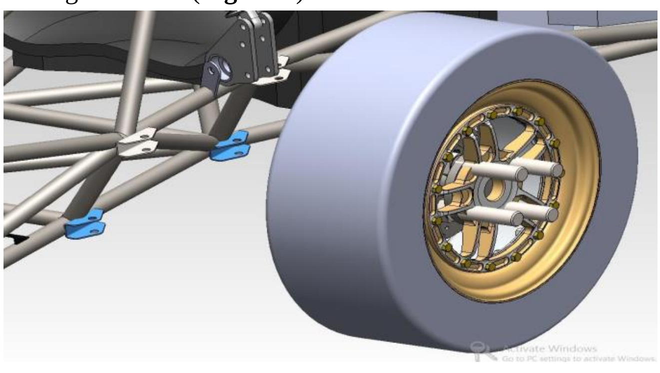

Figure 3: *Repositioning of steering rack*

DESIGN ANALYSIS

Analyzing and resolving the loads, it was found that three major force components were found into the y, x and z axis. The Y- axis force was being negated into the calculations as it is vertical force and assumed to be distributed. The z axis force of 783.7 N is approximated as 800 N for simplicity of analysis. Resolving the x axis and z axis force along the clevis steering and mounting bracket, the outcome is 800 N along horizontal and 461 N at an angle of 30^o as illustrated in **Figure 4**a below.

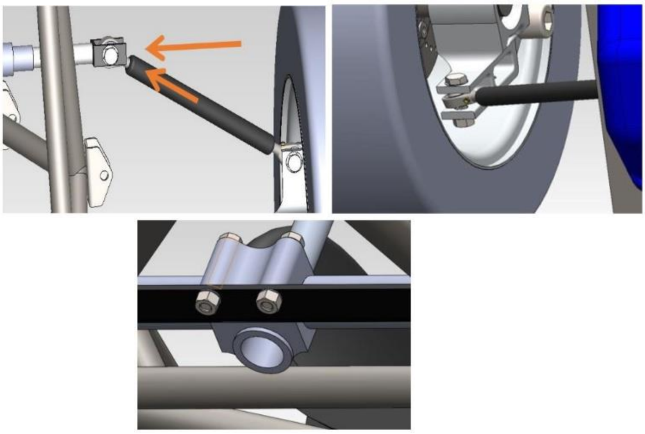

Figure 4: *a) Tie rod and mounting bracket b) M10 bolt c) M8 bolt at rack mounting bracket*

Bolts in the steering arms and rack assemblies were force transfer points, therefore they were subjected to these critical loads. It is found that M10 bolt (**Figure 4**a) in steering arm assembly was subjected to 923.76 N force and both M8 bolts at the rack mounting bracket had received half of this magnitude (figure 4c). However, this applied force is well below the strength of these bolts (22kN and 45kN for M8 and M10 bolts respectively).

FINITE ELEMENT ANALYSIS OF STEERING COMPONENTS

Two 5 mm fillet weld fix the rack mount to the 24.5 mm chromoly frame members. These welds were completed using TIG, argon shielding gas and ER80S-D2 filler metal. The situation is replicated in the ANSYS model. Two temporary 8 mm rods were loaded with the critical cornering load of y:461N and x:800N. Two solids at either end were created to simulate the 5 mm fillet weld. This is depicted in the **Figure 5** below. A mesh refinement of 3 was applied at the weld ends and bolting holes.

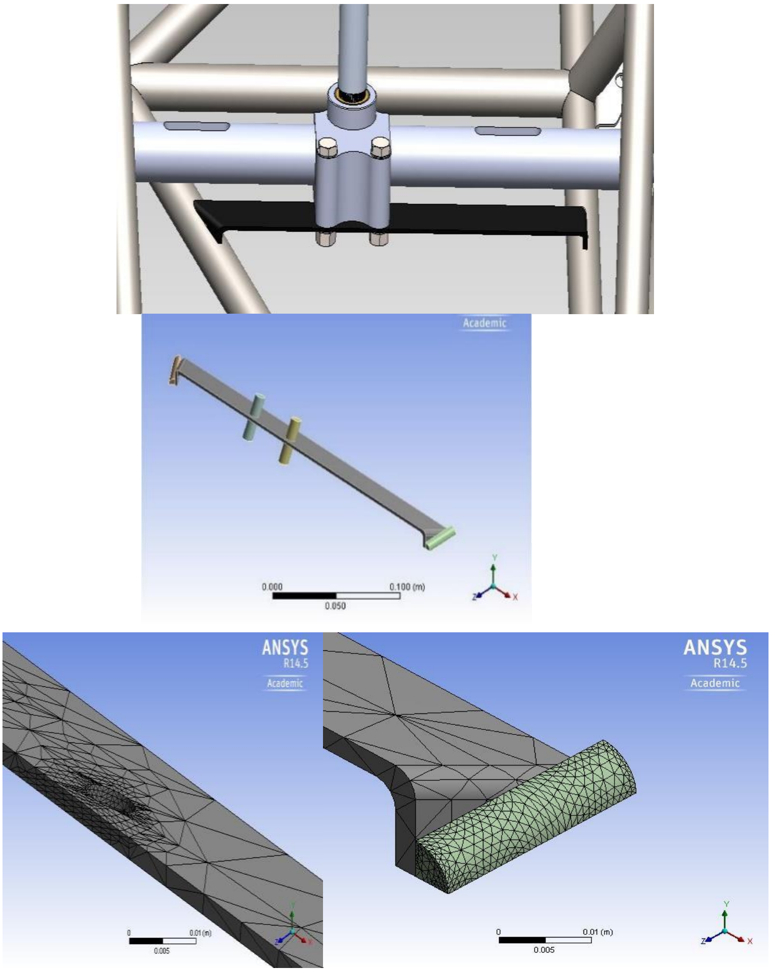

Figure 5:

Figure 5: *Rack mounting bracket welds SOLIDWORKS and ANSYS model*

Hand calculations have estimated a von misses stress equivalent of 5.586 M Pa. However, from the ANSYS analysis it was found that the stress range is between 29.55KPa and 69.97MPa (**Figure 6**). These stresses are well below the yield strength of the ER80S-D2 filler metal at 492MPa. The maximum stress location occurred in the bolt holes with a stress of 314.77MPa. Again, this is within the limits of the yield strength of 4130 chromoly steel. These results imply the selected welds are suitable for fixing the mounting bracket to the frame.

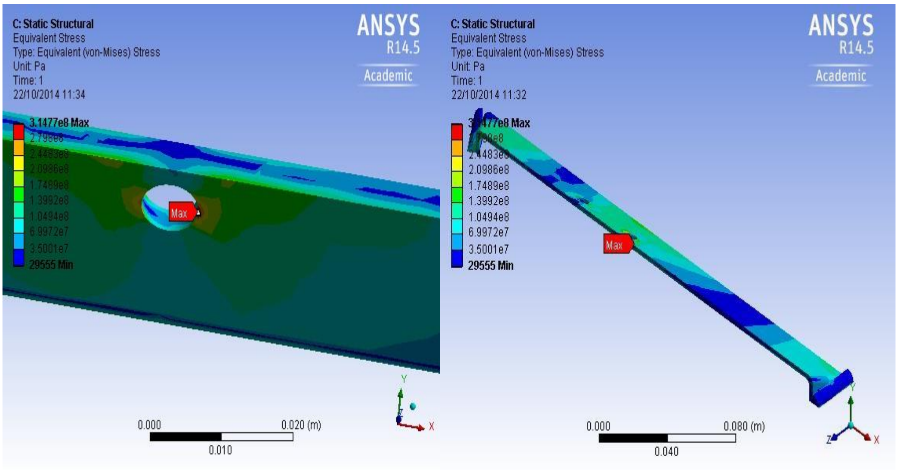

Figure 6: *ANSYS simulation analysis of mounting bracket.*

RACK ARM CLEVIS ANALYSIS

The resultant of x = 800N and Y=461N is 931 N acting on the temporary pin of clevis pin hole with the clevis is being constrained with a fixed support. The clevis design consisted of two 10 mm pin holes with the pin hole plates having a thickness of 3 mm and a 20 mm geometry depth. Its ANSYS analysis is illustrated in **Figure 7** below. The mesh is being refined by a factor of 3 at the critical zones.

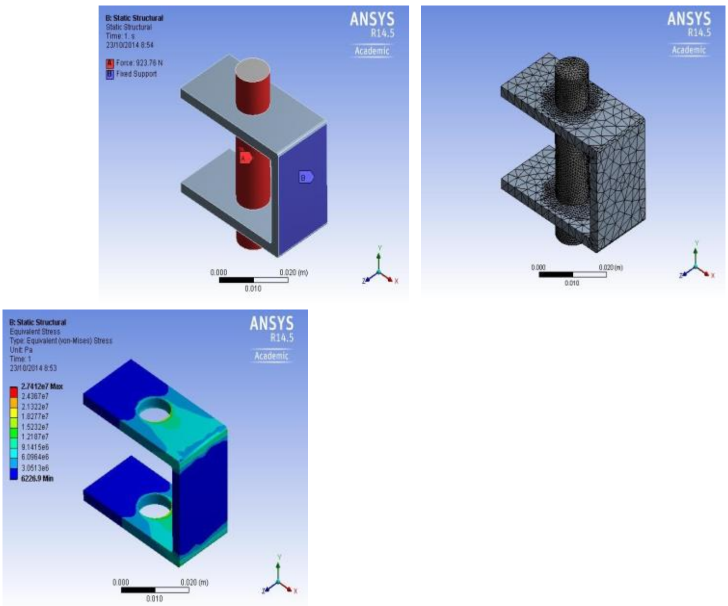

Figure 7: *a) Load and resistance case of clevis (left) b) Mesh case of clevis(middle) c) Static structure analysis(right)*

The result of the equivalent von misses stress analysis of clevis with a 931.76 N load is shown in **Figure 7**c.

Additionally, a fatigue analysis was completed for the clevis using an endurance modifying factor of 0.571. A fully reversed load was assumed and the Goodman stress theory was used as the fatigue criteria. These conditions were used for all fatigue analysis done on the clevis. An image of the life and safety factor for the clevis are shown below is **Figure 8**a and **Figure 8**b.

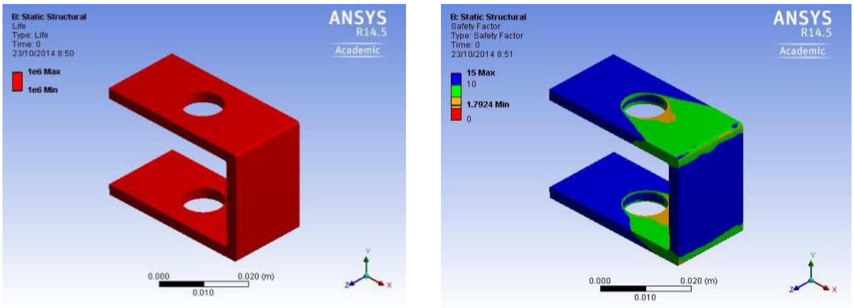

Figure 8: *a) Resultant life plot of clevis(left) b) Resultant safety factor plot of clevis(right)*

A review of the compiled data revealed that the safety factor was in excess of 1 for the entirety of the clevis with a minimum fatigue safety factor of 1.79. Hand calculations reinforce ANSYS data as a fatigue safety factor of 3.48 was calculated for the clevis pin hole. The life plot confirms that the clevis is rated for infinite life under the current loading conditions. As such, the clevis when loaded with the worst possible load case with the contact patch being located in line with the rack arm under cornering loads is rated for infinite life.

RACK ARM ANALYSIS

The steering rack was analyzed as a whole due to the complex geometry of the steering rack and mesh refinement is only applied to areas of interests. The main area of interest for the steering rack arm was the region where the fully extended rack arm meets the steering rack housing and a mesh refinement of 3 was applied in this region as shown in **Figure 9**a.

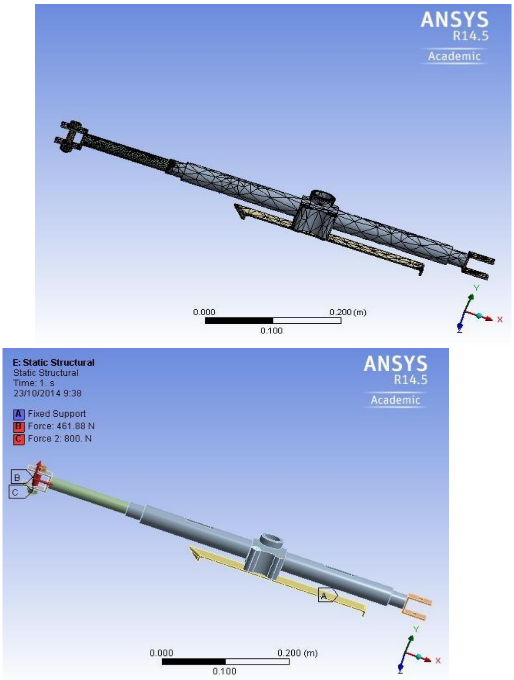

***Figure 9:** Steering rack a) Meshing(left) b) Load and support setup of rack arm(right)*

Similar to the rack arm clevis, the rack arm was analyzed during the worst possible case when the contact patch is in line with the rack arm under corning loads. As such, the clevis bolt on the fully extended rack arm was loaded and the bracket was used to secure the assembly using the fixed support as depicted in **Figure 9**b. The contact region between bolt and washer found to have a maximum von-misses stress of 459 MPa illustrated in **Figure 10**.

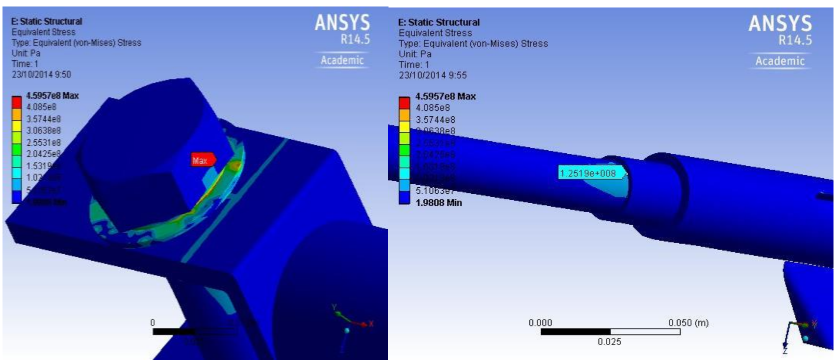

***Figure 10:** Maximum von- misses stress at contact regions*

The equivalent stress at region where the fully extended rack arm meets the steering rack housing have found to have a stress of 125 MPa (**Figure 11**) in comparison of 118 MPa calculated by hand.

Rack arm is also subjected to fully reversed fatigue analysis with the Goodman safety theory as a safety criterion and endurance modifying factor of 0.651. **Figure 11** illustrates the infinite life behavior of rack arm.

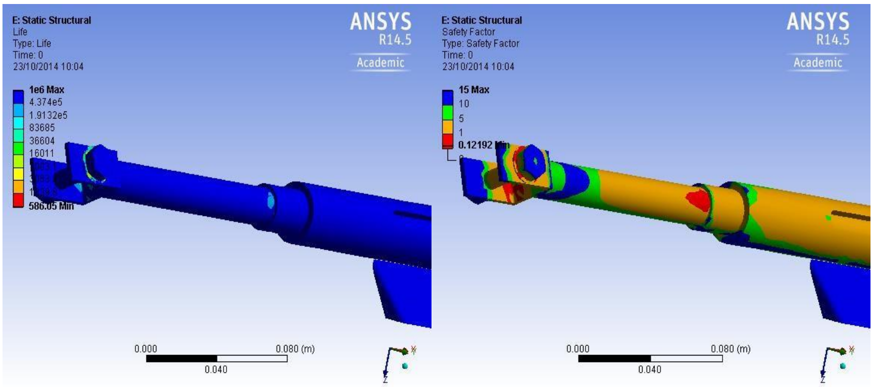

Figure 11: *a) Infinite life plot(left) b) safety factor plot(right)*

As shown in **Figure 11** a, region where the rack arm meets the rack housing can withstand fluctuations ranging 80, 000 to 90, 000 till failure. However, it is highly unlikely that it is subjected to this much fluctuations in its full lifetime.

FINAL DESIGN

The final design can be broken in to three main design components, and is typical to most kart style motor sport steering system.

- Steering column assembly
- Steering rack assembly
- Tie rod assemblies

These assemblies link together to form the final steering system. This is illustrated in the **Figure 12** below

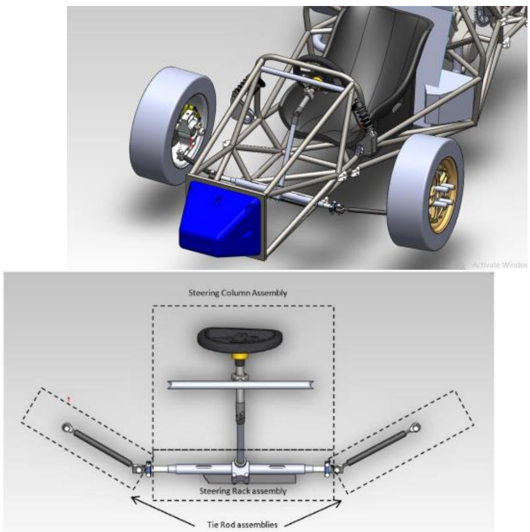

Figure 12: *a) Steering system isometric view(left) b) Steering system main component breakdown(right)*

The design is a standard universal joint, rack and pin steering system where by rotational forces are turned into linear motion from a pinion gear and rack. These forces are then transferred from the tie rods into wheel uprights where turning begins. The steering column is simply supported by a rotational rod end under the front hoop. The column is then spline attached into the rack which is supported at an angle of 21.6^{o}. A clevis at either end links the tie rods through 10mm rods ends. The following **Figure 13** illustrates this final design.

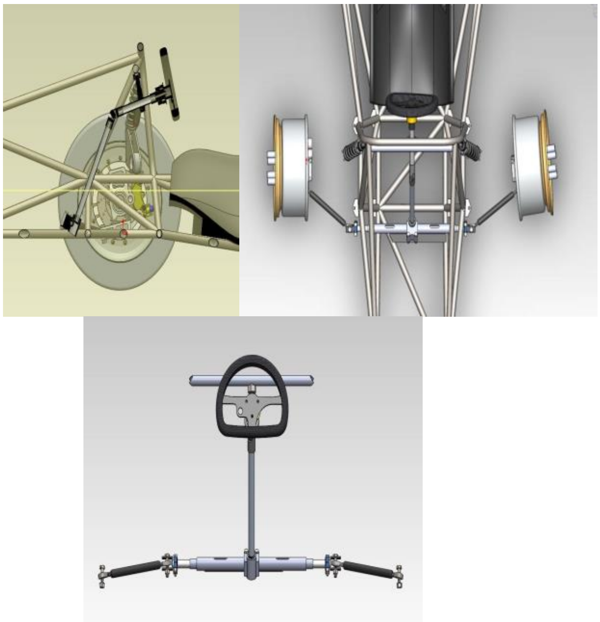

Figure 13: *Steering assembly a) Mid planar view (left) b) Top view with wheel assembly (middle) c) Drivers view(right)*

ASSEMBLY PARTS OF STEERING SYSTEM

SKF SAKAC 10 M ends are selected as rod ends for the steering arm assembly, allowing rigid force transfer between rack arms and upright assembly as well as vertical motion of wheel assembly in operation. In addition, there are attached grease nipples for ease of lubrication(**Figure 14**). In this build a fine 1.25mm pitch thread was selected where the minimum cross sectional area was larger at 61.22mm^2.

Figure 14: *Rod ends a) SKF 10 mm(left) b) SKF 25 mm(right)*

Similarly, an SKF SAKAC 25M rod end was selected as the steering column support permitting a rigid x and y axis platform for the 25mm diameter 162mm steering column to rotate about. Again this rod end uses a 1.25mm fine pitch thread with the thread diameter of 16mm (M16).

The designed rack a 360^{o} rotation of pinion corresponds to 35 mm x displacement of the rack arm. The rack is fabricated with machined aluminum, having arms of 20 mm solid alloy rod and clevises are bolted flush to the ends (**Figure 15**). The rack is mounted using two Class 8.8 M8 Bolts and 4 X 8mm mild steel washers. The splined pinion insert is ¾ inch 19mm 48 splined.

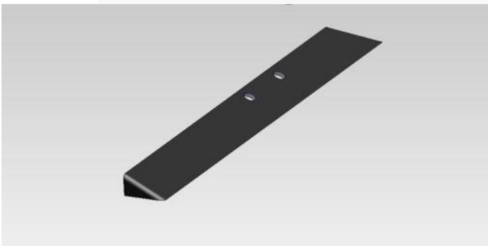

Figure 15: *a) Rack and pinion mechanism(left) b) Mounting bracket(right)*

The mounting bracket (**Figure 15**) for the steering rack was manufactured at JCU Engineering workshop with 3mm plate of 4130 Chromoly steel. The bracket is being welded onto the bottom frame using two 5 mm welds along the outside of bracket contacts. The rack is mounted on the brackets using two class 8.8 M8 bolts and 8mm washers.

M 8 AND M 10 BOLTS AND WASHERS

All bolts in the steering assembly are class 8.8 as per FSAE rules. In the assembly 6 x M8 and 4 x M10 exist with the associated washers and nuts. As per rules a minimum of two threads protrude from the nut trailing end. Information on these bolts and location is tabulated(***Table 1***) and shown(**Figure 16**)below.

Table 1: *Information on bolts*

Nominal Size	Pitch mm	Stress Area mm^2	Min. Tensile Stress MPa	Ult. tensile load kN	Min. Breaking Shear load kN
M8	1.25	36.60	800	29.28	22
M10	1.5	58.00	800	46.60	45

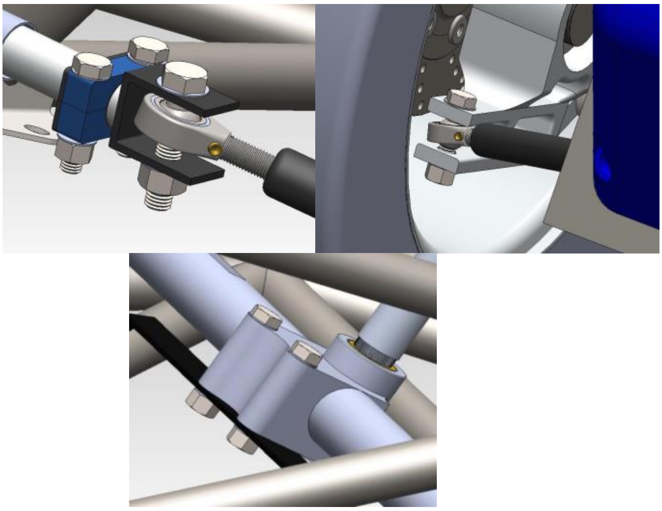

Figure 16: *Location of bolts*

The chosen universal is a ‘no slop’ compact unit with an operating angle operating angle of 35 degrees, which is the angle at which the assembly has been designed for (**Figure 17**a). This blank universal was machined with the following properties from PMD racing products Australia – ¾” – 48 spline x ¾” -48 spline at respective ends. This is having an outer diameter of 28mm and Inner major diameter 19mm with a 25 mm bore of each internal spline.

Figure 17: *a) Universal joint(left) b) 325 mm steering column(right) c) 162 mm steering column(middle)*

Two splined steering columns was machined in order to complete the steering column assembly (**Figure 17**a & b). A 162mm length column and 325mm column was machined from chromyl with a ¾” 48 spline 9mm splined end with a spline length of 25mm. The diameter of these shafts is 25mm with an inside diameter of 18mm.

LOCKING COLLARS

In order to stop the clevis colliding with the steering with the rack on full lock and to restrict the steering of the vehicle two locking collars were manufactured. The design consisted of two 12mm wide top and bottom pieces which when assembled allowed a 20mm rod to be inserted. This is where the rack arm will connect. Two M8 bolts were holding the two parts together and provided locking forces to the rack arm. To reduce any possible damage to the arm, a thin 1mm copper sleeve was inserted into the hole made from copper sheeting. This had also distribute clamping forces. An assembled and exploded view of the locking collars is depicted in **Figure 18** below

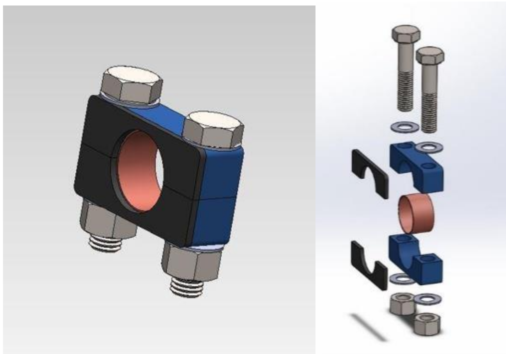

***Figure 18**: Assembled(left) and exploded view(right) of locking collars*

TECHNICAL SPECIFICATIONS

Ultimately the final design had to meet the requirements of the initial design constraints and perform these actions within the FSAE rules. The top plane view below illustrates some of the geometrical relations between the steering rack and tie rod assemblies(**Figure 19**).

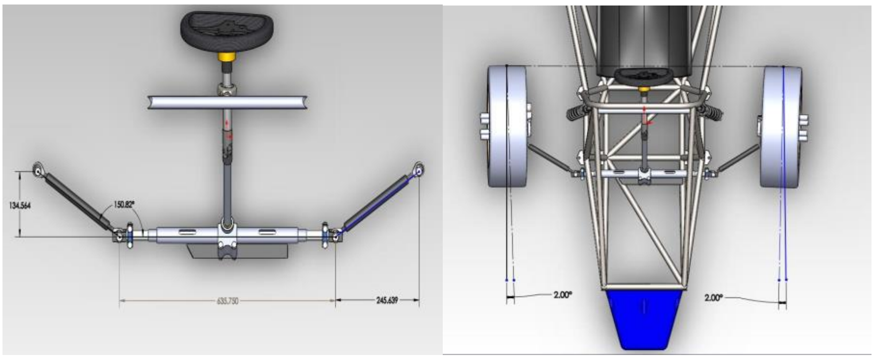

***Figure 19:** a) Top view geometric relations of steering system(left) b) Toe in reference dimensions(right)*

Note that this shows the geometric relations when the rack is in a neutral position, with the Toe. The current configuration has a U-joint operating angle of 34.5^{o}. Which is in the range of the joint specification. Furthermore, the steering column support bar has been designed so that minor corrections can be made to this angle. By simply removing the 162mm steering column and rotating the support rod end, the steering wheel can shift 12mm vertically, relieving the angle further.

ERGONOMIC FACTORS

- Leg clearance from frame base = 54.710mm
- Steering wheel angle approx. = 16^{o}
- Universal Joint clearance = 335.8 mm
- Column support clearance = 368.7mm

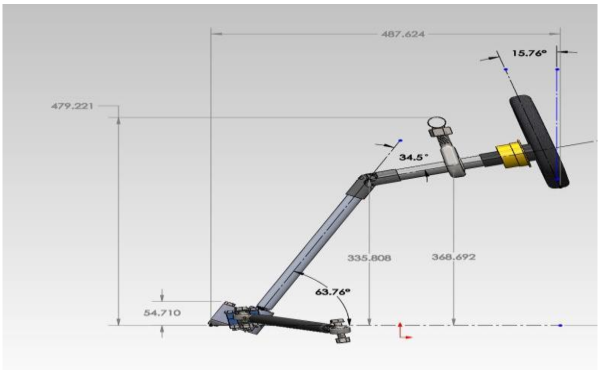

Figure 20: *Side view geometric relations*

Leaving the universal joint angle at 34.5^{o} (shown in **Figure 20**) was desired as suppressing the angle further would require shifting the rack further forward in the frame. Doing so would reduce the space allowed for the complex foot pedal/ control assemblies that are required in the vehicle.

CONCLUSION

Using the proposed constraints, an appropriate steering system was devised as an improvement in regards to the previous generation. The universal joint operating angle was relieved to a suitable degree as specified in the chosen joint. A major design component was to mitigate the lag in steering induced by the previous locking pin system in the steering column assembly. This was investigated, and appropriate splined components were designed where necessary, however the inclusion of splined parts incurs higher manufacturing costs.

FEA analysis concluded that all critical components are well within operating constraints of the critical load case proposed under fatigue, and static analysis. The final design was commended with an appropriate turning radius, using the existing rack. Collaboration with the suspension, uprights, A-arm/wishbone assembly teams is needed to effectively coordinate a solution.

REFERENCES

[1] Okada T, Imura T, Shimizu T. Smart one-hand operation mechanism for multi-purpose steering of a four-wheeled vehicle. vol. 6. IFAC; 2007. doi:10.3182/20070903-3-FR-2921.00059.

[2] Lloyd JE. Vehicle Standard (Australian Design Rule 10 / 01 – Steering Column) 2006 2006:1–51.

[3] Reinelt W, Klier W, Lundquist C, Reirnann G, Schuster W, Groβheim R. Active Front Steering for Passenger Cars: System Modelling and Functions. IFAC Proc Vol 2004;37:679–84. doi:10.1016/s1474-6670(17)30422-6.

[4] Vangi D, Virga A, Gulino MS. Combined activation of braking and steering for automated driving systems: Adaptive intervention by injury risk-based criteria. Procedia Struct Integr 2019;24:423–36. doi:10.1016/j.prostr.2020.02.039.

[5] Kurebwa J, Mushiri T. Design and simulation of an integrated steering system for all-purpose Sport Utility Vehicles (SUVs) - Case for Toyota. Procedia Manuf 2019;35:56–74. doi:10.1016/j.promfg.2019.07.002.

[6] Gao Z, Wang J, Wang D. Dynamic modeling and steering performance analysis of active front steering system. Procedia Eng 2011;15:1030–5. doi:10.1016/j.proeng.2011.08.190.

[7] Pereira Dos Santos S, Cardoso Brandão L, Henrique Gallicchio L, De Castro Silveira Z. Finishing process analysis between honing and hard hobbing in pinion gears applied to a steering system. Energy Procedia 2012;14:2–8. doi:10.1016/j.egypro.2011.12.888.

[8] Land MF, Tatler BW. Steering with the head. Curr Biol 2001;11:1215–20. doi:10.1016/s0960-9822(01)00351-7.

[9] Khristamto M, Praptijanto A, Kaleg S. Measuring geometric and kinematic properties to design steering axis to angle turn of the electric golf car. Energy Procedia 2015;68:463–70. doi:10.1016/j.egypro.2015.03.278.

[10] Saurabh YS, Kumar S, Jain KK, Behera SK, Gandhi D, Raghavendra S, et al. Design of Suspension System for Formula Student Race Car. Procedia Eng 2016;144:1138–49. doi:10.1016/j.proeng.2016.05.081.

NOTIFICATION TO AUTHORS

The Journal MVM publishes original papers which have not been previously published in other journals. This is responsibility of the author. The authors agree that the copyright for their article is transferred to the publisher when the article is accepted for publication.

The language of the Journal is English.

Journal ***Mobility & Vehicles Mechanics*** is at the SSCI list.

All submitted manuscripts will be reviewed. Entire correspondence will be performed with the first-named author.

Authors will be notified of acceptance of their manuscripts, if their manuscripts are adopted.

INSTRUCTIONS TO AUTHORS AS REGARDS THE TECHNICAL ARRANGEMENTS OF MANUSCRIPTS:

Abstract is a separate Word document, "*First author family name_ABSTRACT.doc*". Native authors should write the abstract in both languages (Serbian and English). The abstracts of foreign authors will be translated in Serbian.

This document should include the following: 1) author's name, affiliation and title, the first named author's address and e-mail – for correspondence, 2) working title of the paper, 3) abstract containing no more then 100 words, 4) abstract containing no more than 5 key words.

The manuscript is the separate file, „*First author family name_Paper.doc*" which includes appendices and figures involved within the text. At the end of the paper, a reference list and eventual acknowledgements should be given. References to published literature should be quoted in the text brackets and grouped together at the end of the paper in numerical order.

Paper size: Max 16 pages of B5 format, excluding abstract
Text processor: Microsoft Word
Margins: left/right: mirror margin, inside: 2.5 cm, outside: 2 cm, top: 2.5 cm, bottom: 2 cm
Font: Times New Roman, 10 pt
Paper title: Uppercase, bold, 11 pt
Chapter title: Uppercase, bold, 10 pt
Subchapter title: Lowercase, bold, 10 pt
Table and chart width: max 125 mm
Figure and table title: Figure _ (Table _): Times New Roman, italic 10 pt

Manuscript submission: application should be sent to the following e-mail:

mvm@kg.ac.rs ; lukicj@kg.ac.rs
or posted to address of the Journal:
University of Kragujevac – Faculty of Engineering
International Journal M V M
Sestre Janjić 6, 34000 Kragujevac, Serbia

The Journal editorial board will send to the first-named author a copy of the Journal offprint.

OBAVEŠTENJE AUTORIMA

Časopis MVM objavljuje orginalne radove koji nisu prethodno objavljivani u drugim časopisima, što je odgovornost autora. Za rad koji je prihvaćen za štampu, prava umnožavanja pripadaju izdavaču.

Časopis se izdaje na engleskom jeziku.

Časopis ***Mobility & Vehicles Mechanics*** se nalazi na SSCI listi.

Svi prispeli radovi se recenziraju. Sva komunikacija se obavlja sa prvim autorom.

UPUTSTVO AUTORIMA ZA TEHNIČKU PRIPREMU RADOVA

Rezime je poseban Word dokument, "*First author family name_ABSTRACT.doc*". Za domaće autore je dvojezičan (srpski i engleski). Inostranim autorima rezime se prevodi na srpski jezik. Ovaj dokument treba da sadrži: 1) ime autora, zanimanje i zvanje, adresu prvog autora preko koje se obavlja sva potrebna korespondencija; 2) naslov rada; 3) kratak sažetak, do 100 reči, 4) do 5 ključnih reči.

Rad je poseban fajl, „*First author family name_Paper.doc*" koji sadrži priloge i slike uključene u tekst. Na kraju rada nalazi se spisak literature i eventualno zahvalnost. Numeraciju korišćenih referenci treba navesti u srednjim zagradama i grupisati ih na kraju rada po rastućem redosledu.

Dužina rada: Najviše 16 stranica B5 formata, ne uključujući rezime
Tekst procesor: Microsoft Word
Margine: levo/desno: mirror margine; unurašnja: 2.5 cm; spoljna: 2 cm, gore: 2.5 cm, dole: 2 cm
Font: Times New Roman, 10 pt
Naslov rada: Velika slova, bold, 11 pt
Naslov poglavlja: Velika slova, bold, 10 pt
Naslov potpoglavlja: Mala slova, bold, 10 pt
Širina tabela,dijagrama: max 125 mm
Nazivi slika, tabela: Figure __ (Table _): Times New Roman, italic 10 pt

Dostavljanje rada elektronski na E-mail: **mvm@kg.ac.rs ; lukicj@kg.ac.rs**

ili poštom na adresu Časopisa
Redakcija časopisa M V M
Fakultet inženjerskih nauka
Sestre Janjić 6, 34000 Kragujevac, Srbija

Po objavljivanju rada, Redakcija časopisa šalje prvom autoru jedan primerak časopisa.

MVM *Editorial Board*
University of Kragujevac
Faculty of Engineering
Sestre Janjić 6, 34000 Kragujevac, Serbia
Tel.: +381/34/335990; Fax: + 381/34/333192
www.mvm.fink.rs